

LIBRARY
UNIVERSITY OF MORATUWA, SRI LANKA
MORATUWA

LB/DON/40/2011

DEE 05179

**MODELING OF POWER TRANSMISSION
LINES FOR LIGHTNING BACK
FLASHOVER ANALYSIS
A CASE STUDY: 220kV BIYAGAMA -
KOTMALE TRANSMISSION LINE**

Master of Science Dissertation

M.CHANAKA

**Department of Electrical Engineering
University of Moratuwa, Sri Lanka**

621.3"10"

621.3(043)

TH

December 2010

96441

University of Moratuwa



96441

96441



**MODELING OF POWER TRANSMISSION LINES
FOR LIGHTNING BACK FLASHOVER
ANALYSIS
A CASE STUDY: 220KV BIYAGAMA - KOTMALE
TRANSMISSION LINE**

A dissertation submitted to the Department of Electrical Engineering,
University of Moratuwa in partial fulfillment of the requirement for the
Degree of Master of Science

by

MALLIKARACHCHIGE CHANAKA

Supervised by: Prof. H.Y.R. Perera

Eng. K.P.K. Shanthi

**Department of Electrical Engineering
University of Moratuwa, Sri Lanka**

December 2010

DECLARATION

The work submitted in this dissertation is the result of my own investigation, except where otherwise stated.

It has not already been accepted for any degree, and is also not being concurrently submitted for any other degree.

.....

M. Chanaka

30th December 2010

We endorse the declaration by the candidate.

UOM Verified Signature

Prof. H.Y.R. Perera

.....

Eng. K.P.K. Shanthi

CONTENTS

Declaration.....	i
Abstract.....	v
Dedication.....	vi
Acknowledgement.....	vii
List of Figures.....	viii
List of Tables.....	x

CHAPTER - 1..... 1

Introduction..... 1

1.1 Historical overview of lightning	1
1.2 The lightning phenomena.....	2
1.2.1 Charge separation of thunder clouds	2
1.2.2 Electric fields and energy in thunder clouds	3
1.2.3 Leader formation and breakdown mechanism.....	4
1.2.4 Types of lightning.....	5
1.2.5 Frequency of occurrence of lightning.....	5
1.3 Lightning data of Sri Lanka	5
1.4 Introduction to transmission system of Sri Lanka.....	6
1.5 Lightning effects on power transmission lines.....	7
1.6 Lightning Parameters	9
1.6.1 The quantity of lightning activity in a given area.....	9
1.6.2 The distribution of the crest current of a lightning flash	9
1.6.3 The wave shape of a lightning flash	10
1.6.4 Total charge delivered by a lightning stroke	10
1.7 Selected transmission line for the study.....	11
1.7.1 Transmission Towers and configuration	12
1.7.2 Insulators and arc horn gaps	13
1.7.3 Phase conductors	13
1.7.4 Earthing of towers	13

CHAPTER - 2..... 15

Problem identification

2.1 Introduction	15
2.2 Preliminary studies.....	15
2.2.1 The relationship between monthly Isokeraunic level and line failures	16
2.2.2 Line sections having higher probability of insulator failures	17
2.3 Back flashover effects on transmission lines	17
2.3.1 Earth faults at power frequency voltage due to back flashover events	18
2.4 Prevention of Back flashover events.....	18
2.5 Project objectives	19

CHAPTER - 3	20
Methodology	20
3.1 EMTP/PSCAD modeling and simulation	20
3.2 Proposed electromagnetic transient model for 220kV Biyagama-Kotmale transmission line.....	21
3.3 Electromagnetic fast front transient sub models for transmission line elements	22
3.3.1 Frequency dependent (Phase) model representing Transmission line sections and spans.....	22
3.3.2 Loss-Less Constant Parameter Distributed Line (CPDL) model representing the transmission towers	23
3.3.3 Tower grounding resistance model.....	25
3.3.4 Line insulators and back flashover model	26
3.3.5 Line termination model	28
3.3.6 Surge arrester model.....	29
3.3.7 Lightning stroke current generator model	31
3.3.8 Power frequency phase voltage generator model	33
3.4 Selection of a Transmission Line Arrester (TLA)	34
CHAPTER - 4	36
Application of the methodology	36
4.1 Introduction	36
4.2 Power Systems CAD (PSCAD) modeling tool	36
4.2.1 PSCAD Graphical User Interface (GUI) window	36
4.3 Creation of sub models in PSCAD.....	38
4.3.1 Transmission line model.....	38
4.3.2 Transmission tower model.....	40
4.3.3 Tower grounding resistance model.....	40
4.3.4 Line insulator string with back flashover model	41
4.3.5 Power frequency phase voltage generator model	42
4.3.6 Line end termination model.....	43
4.3.7 Surge Arrester model.....	43
4.3.8 Lightning surge generator model.....	48
4.4 Assembly of sub models and data signal coordination	49
4.5 Method of simulation	49
4.5.1 Multiple Run component and variable settings	49
4.5.2 Simulation criteria	51
4.5.3 Project simulation settings.....	53
CHAPTER - 5	54
Results and analysis	54
5.1 Introduction	54

5.2 Back flashover minimum current variation results and analysis.....	55
5.2.1 Results of simulations without arrester protection (Step-1)	55
5.2.2 Results of simulations with arrester protection (Step-2)	58
CHAPTER - 6.....	62
Conclusion and recommendations	62
6.1 Conclusion.....	62
6.2 Recommendations	62
REFERENCES.....	63
Annex-1 Present Transmission system of Sri Lanka	A1
Annex-2 Transmission system of Sri Lanka (Single line diagram).....	A2
Annex-3 220kV Biyagama – Kotmale transmission line parameters.....	A3
Annex-4: A typical transmission tower used in the selected transmission line	A4
Annex-5: Tower schedule	A5
Annex-6 Grounding Resistance variation of towers due to soil ionization effect	A6
Annex-7 Simplified selection procedure of an ABB surge arrester	A7-1

Abstract

Performance of power transmission lines has a great impact on reliability aspects of a particular power supply system of a country. Unreliable power transmission lines can even lead to total power failures resulting with great financial losses. The lightning back flashover effects are recognized as one of the major causes of transmission line outages.

Several types of solutions are presently available to address the issue of lightning back flashovers. However the modern concept of transmission line mounted surge arresters is of great popularity due to its excellent performance, ease of installation and the low cost compared to the other traditional solutions.

This report describes a case study which was carried out on one of critical 220kV power transmission lines of the Sri Lankan transmission network, having several past records of lightning back flashover related outages resulting with total system failures.

The study described in this report is mainly focuses on the way of analyzing the back flashover events by transient modeling and subsequent simulation of the selected transmission line in an electromagnetic transient computer program. The study uses the Power System CAD (PSCAD) software program as the software tool for the purpose of modeling and simulation of selected 220kV Biyagama-Kotmale power transmission line.

Simulation of the created transmission line model is carried out with and without Transmission Line Arrester (TLA) model to evaluate the improvements in lightning back flashover performance after installation of TLAs in the selected transmission line.

The result of the simulations shows that the installation of 02nos.of TLAs at top phases of each selected towers improves the lightning performance of the selected power transmission line.

Acknowledgement

Thanks are due first to my supervisors, Professor H.Y.R. Perera and Eng. K.P.K. Shanthi, for their great insights, perspectives, guidance and sense of humor. My sincere thanks goes to the officers in the Post Graduate Office, Faculty of Engineering, University of Moratuwa, Sri Lanka for helping in various ways to clarify the things related to my academic works in time with excellent cooperation and guidance. Sincere gratitude is also extended to the course coordinators and rest of the staff who serve in the Department of Electrical Engineering office.

My special thanks goes to Dr. Dharshana Muthumuni who spent his valuable time to guide me and providing valuable information required for this study.

I would like to express my sincere gratitude to Eng. L.A.S. Fernando, Eng. (Mrs.) N Amarasiri, Eng. W.W.R. Pitawala, Eng. W.D.A.J. Chandrakumara, Eng. N.L.A.A. Chandranath, Eng. W.A. Jayalath and Eng. U. Ranathunga working at Ceylon Electricity Board for their excellent support and the encouragement towards the success of this academic work.

Further my heartfelt thanks goes to Eng. L.A.A.N. Perera, Eng. K.P.D.S.K. Dharmadasa and Eng. D.L.P. Munasinghe for their valuable help and the continuous encouragement.

Finally, I would like to thank many individuals, friends and colleagues who have not been mentioned here personally in making this educational process a success. I could not be able to done it without your support.

M.Chanaka

29th December 2010

List of figures

Figure	Description	Page
Figure 1.1	– Benjamin Franklin’s famous kite experiment in 1752	1
Figure 1.2	– Charge distribution of thunder clouds and types of lightning	2
Figure 1.3	– Progression of the Downward Leader and formation of the Return Stroke	4
Figure 1.4	– Isokeraunic Level (IKL) map of Sri Lanka [5]	6
Figure 1.5	– Induced charges on a power transmission line	7
Figure 1.6	– Lightning Stroke Current Probability Distribution [6].....	10
Figure 1.7	– 220kV, Biyagama-Kotmale Transmission Line	11
Figure 1.8	– Single line diagram of Victoria complex with Biyagama-Kotmale line .	12
Figure 1.9	– Grounding resistance variation of towers 31-52 and 83-97 starting from Kotmale end.....	14
Figure 2.1	– Comparison of monthly line failures with IKL	16
Figure 3.1	– Complete transmission line model proposed for the analysis	21
Figure 3.2	– Frequency Dependent (Phase) Model in PSCAD and its connection arrangement	22
Figure 3.3	– Constant Parameter Distributed Line (CPDL) Model for Towers	23
Figure 3.4	– Flashover voltage-time characteristic of 220kV line insulation with 2m Arc-horn gap.....	27
Figure 3.5	– Insulator string and back flashover model.....	27
Figure 3.6	– Basic logic diagram for back flashover control module.....	28
Figure 3.7	– Grounding arrangement of a typical end termination model.....	28
Figure 3.8	– Frequency dependent surge arrester model	29
Figure 3.9	– V-I Relationship for nonlinear resistors A_0 and A_1 [12]	30
Figure 3.10	– Standard waveforms for lightning surge voltage and current	32
Figure 3.11	– System and Arrester parameter matching configuration [13]	34
Figure 3.12	– Selection procedure of electrical parameters for ABB surge arresters [13].....	35
Figure 4.1	– Typical working window of PSCAD software.....	37
Figure 4.3	– Transmission line parameter input window	38
Figure 4.2	– Transmission line model (Remote end method).....	38
Figure 4.5	– Typical tower model created in PSCAD	39
Figure 4.4	– General Line Geometry Data input	39
Figure 4.7	– Insulator string capacitor and Back flashover Breaker models	40
Figure 4.6	– Tower grounding resistance model	40
Figure 4.8	– Back flashover control module implemented in PSCAD.....	41
Figure 4.9	– Power frequency phase voltage generator model	42
Figure 4.10	– Line termination model created in PSCAD.....	43
Figure 4.11	– Surge arrester model created in PSCAD	44

Figure 4.12 – Created test circuit in PSCAD for surge arrester testing	45
Figure 4.13 – Test surge waveform 30/60us with 1kA peak	46
Figure 4.14 – Test result, arrester discharge voltage at 1kA	46
Figure 4.15 – Test surge waveform 8/20μs with 10kA peak.....	47
Figure 4.16 – Test result, arrester discharge voltage at 10kA	47
Figure 4.16 – Test result, arrester discharge voltage at 10kA	48
Figure 4.17 – Lightning surge generator model created in PSCAD	48
Figure 4.18 – Multiple Run simulation component in PSCAD.....	49
Figure 5.1 – Typical view of an output data file.....	54
Figure 5.2 – Results of simulation no.1	55
Figure 5.4 – Results of simulation no. 2	56
Figure 5.3 – Results of simulation no. 4	56
Figure 5.5 – Results of simulation no. 5	57
Figure 5.6 – Results of simulation no. 3	57
Figure 5.7 – Results of simulation no. 6	58
Figure 5.8 – Results of simulation no. 7	58
Figure 5.9 – Results of Simulation no. 8	59
Figure 5.11 – Results of Simulation no. 12	60
Figure 5.10 – Results of Simulation no. 11	60



Figure 4.12 – Created test circuit in PSCAD for surge arrester testing	45
Figure 4.13 – Test surge waveform 30/60us with 1kA peak	46
Figure 4.14 – Test result, arrester discharge voltage at 1kA	46
Figure 4.15 – Test surge waveform 8/20μs with 10kA peak	47
Figure 4.16 – Test result, arrester discharge voltage at 10kA	47
Figure 4.16 – Test result, arrester discharge voltage at 10kA	48
Figure 4.17 – Lightning surge generator model created in PSCAD	48
Figure 4.18 – Multiple Run simulation component in PSCAD	49
Figure 5.1 – Typical view of an output data file	54
Figure 5.2 – Results of simulation no.1	55
Figure 5.4 – Results of simulation no. 2	56
Figure 5.3 – Results of simulation no. 4	56
Figure 5.5 – Results of simulation no. 5	57
Figure 5.6 – Results of simulation no. 3	57
Figure 5.7 – Results of simulation no. 6	58
Figure 5.8 – Results of simulation no. 7	58
Figure 5.9 – Results of Simulation no. 8	59
Figure 5.11 – Results of Simulation no. 12	60
Figure 5.10 – Results of Simulation no. 11	60



List of tables

Table	Description	Page
Table 1.1	– Range of values for lightning parameters [6].....	8
Table 1.2	– CEB Specifications for a single insulator disc [4].....	13
Table 2.1	– Monthly line failures and IKL.....	16
Table 3.1	– Calculated parameters for a typical tower model	25
Table 4.1	– Initial I, V values for A_0 and A_1 [11]	45
Table 4.2	– Range of values used for variables in Multiple Run component	50
Table 4.3	– Detailed simulation criteria for Step-1.....	52
Table 4.4	– Detailed simulation criteria for Step-2.....	53



University of Moratuwa, Sri Lanka.
Electronic Theses & Dissertations
www.lib.mrt.ac.lk

Chapter - 1

Introduction

1.1 Historical overview of lightning

In June 1752, an American scientist called Benjamin Franklin (1706–1790) discovered the lightning as a natural phenomenon associated with discharging static electricity by his famous kite experiment accompanied by his son as an assistant (Shown in Figure 1.1).



Figure 1.1 – Benjamin Franklin’s famous kite experiment in 1752

As he discovered, the lightning is a natural phenomenon involving an atmospheric discharge of electricity accompanied by thunder, which typically occurs during thunder storms, and sometimes during volcanic eruptions or dust storms. These lightning strike leaders or in other words a heavy bunch of electric charges can reach travelling speeds about $10,000\text{ms}^{-1}$ and can form extremely high temperatures like $30,000^{\circ}\text{C}$ forming some frightening as well as fascinating events. It has been found in many researchers that there are around 16million lightning storms likely to be formed in the world every year.

The history of lightning is likely to be present even back in billion years ago where the life was not even evolved on our planet. Further it had been possible that the lightning involved in forming some organic molecules necessary for the formation of every life form [1].Harland and Hacker (1966) reported on a fossil glassy tube, referred to as a fulgurite, created by lightning 250million years ago [1].

Even though the Benjamin Franklin had showed that the lightning is a discharge of static electricity; the development of theoretical understanding was rises as the field of power engineering came in to practice, where the power transmission and distribution lines were severely affected by lightning. As a result there were lot of experiments on lightning and in 1900, Nikola Tesla generated artificial lightning by using a large Tesla coil, enabling the generation of enormously high voltages sufficient to create lightning.

1.2 The lightning phenomena

The present scientific explanation on how the lightning is formed is basically developed from the researches carried out by B.F.J. Schonland, D.J.Malan, and their co-workers in South Africa during the 1930s by facilitating a special camera called Streak Camera. It was shown conclusively by the South African researches that lightning strokes lowering negative charge to ground are composed of a downward leader and an upward return stroke and that the first stroke-leader is stepped. B.F.J. Schonland (1956) summarized the main results of the South African studies and much of the presently used lightning terminology was introduced by those studies [1].

1.2.1 Charge separation of thunder clouds

The very first process of generating lightning is considered as the charge separation in a thunder cloud. There are two hypotheses describing the process of charge separation in a thunder cloud called “Polarization mechanism” and “Electrostatic induction”.

The Polarization mechanism has two sub components as mentioned below.

- Falling droplets of ice and rain become electrically polarized as they fall through the atmosphere's natural electric field.
- Colliding ice particles become charged by electrostatic induction.

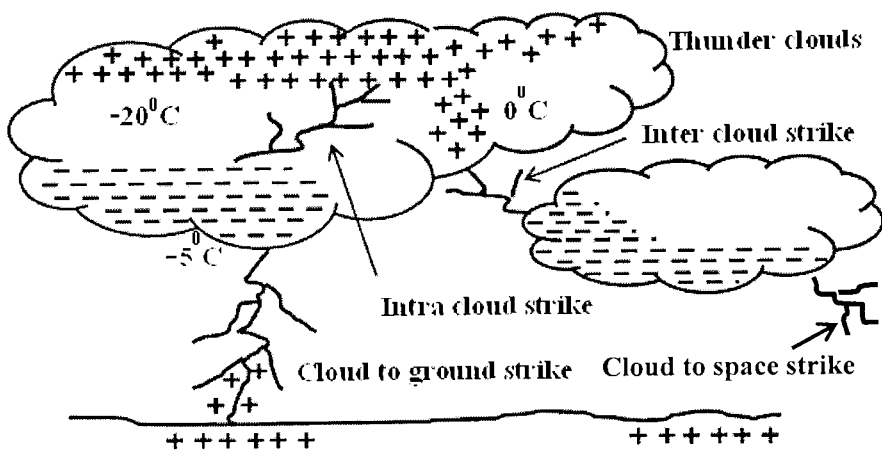


Figure 1.2 – Charge distribution of thunder clouds and types of lightning

Ice and super-cooled water are the keys to the process. Turbulent winds move violently these super-cooled water droplets, causing them to collide. When the super-cooled water droplets hit ice crystals, some negative ions transfer from one particle to

another. The smaller, lighter particles lose negative ions and become positive; the larger, more massive particles gain negative ions and become negatively charged.

According to the electrostatic induction hypothesis charge separation appears to require strong updrafts which carry water droplets upward, super-cooling them to between -10 and -20°C . These collide with ice crystals to form a soft ice-water mixture called Graupel. The collisions result in a slight positive charge being transferred to ice crystals and a slight negative charge to the Graupel. Updrafts drive lighter ice crystals upwards, causing the cloud top to accumulate increasing positive charge. The heavier negatively charged Graupel falls towards the middle and lower portions of the cloud, building up an increasing negative charge. Charge separation and accumulation continue until the electrical potential becomes sufficient to initiate lightning discharges, which occurs when the gathering of positive and negative charges forms a sufficiently strong electric field.

Therefore due to charge separation process, in most of the thunder clouds there is a Negative Charge Centre at the bottom of the cloud where the temperature is about -5°C , whereas Positive Charge Centre appears at the top of the cloud at temperature about -20°C . In addition to these there are localized positively charged region formed near the base of the cloud where the temperature is about 0°C .

1.2.2 Electric fields and energy in thunder clouds

In a typical thunder cloud, the static charge of about 20C are separated by distances of about 3km whereas a field of about 1000V/m is existing near the center of the cloud giving a total potential difference between the charge centres to be between 100 to 1000MV . Therefore this type of charged cloud is capable of dissipating energy of the order of 1000 to $10,000\text{MJ}$ by a lightning stroke where much of the energy is spent in heating up a narrow air column surrounding the discharge to a temperature is about $15,000^{\circ}\text{C}$ within few microseconds [3].

Basically the static charge content of a bipolar charged cloud is in the range of 10 to 30C whereas the charge centres are separated by a distances in the range of 2 to 5km . The average current dissipated by lightning is of the order of kilo-amperes. During an average lightning storm, a total of the order of kilo-coulombs of charge would be generated, between the 0°C and the -40°C levels, in a volume of about 50km^3 [3].

1.2.3 Leader formation and breakdown mechanism

As a thundercloud moves over the Earth's surface, an equal but opposite charge is induced in the Earth below, and the induced ground charge follows the movement of the cloud. An initial bipolar discharge, or path of ionized air, starts from a negatively charged mixed water and ice region in the thundercloud. The discharge ionized channels are called leaders. The negative charged leaders, called a "stepped leader", proceed generally downward in a number of quick jumps, each up to 50 meters long (See Figure 1.3). Along the way, the stepped leader may branch into a number of paths as it continues to descend. The progression of stepped leaders takes a comparatively long time (hundreds of milliseconds) to approach the ground. This initial phase involves a relatively small electric current (tens or hundreds of amperes), and the leader is almost invisible compared to the subsequent lightning channel.

When a stepped leader approaches the ground, the presence of opposite charges on the ground enhances the electric field. The electric field is highest on trees and tall buildings. If the electric field is strong enough, a conductive discharge (called a positive streamer) can develop from these points. As the field increases, the positive streamer may evolve into a hotter, higher current leader which eventually connects to the descending stepped leader from the cloud. It is also possible for many streamers to develop from many different objects simultaneously, with only one connecting with the leader and forming the main discharge path. When the two leaders meet, the electric current greatly increases. The region of high current propagates back up the

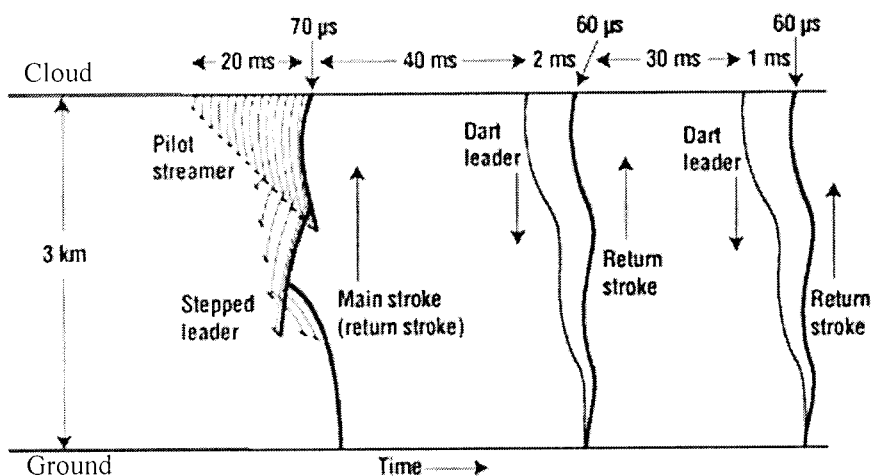


Figure 1.3 – Progression of the Downward Leader and formation of the Return Stroke

positive stepped leader into the cloud with a "return stroke" that is the most luminous part of the lightning discharge.

When the electric field becomes strong enough, an electrical discharge (the bolt of lightning) occurs within clouds or between clouds and the ground. During the strike, successive portions of air become a conductive discharge channel as the electrons and positive ions of air molecules are pulled away from each other and forced to flow in opposite directions. The electrical discharge rapidly superheats the discharge channel, causing the air to expand rapidly and produce a shock wave heard as thunder. The rolling and gradually dissipating rumble of thunder is caused by the time delay of sound coming from different portions of a long stroke.

1.2.4 Types of lightning

Currently there are few number of major lightning types have been recognized based on particular characteristics exhibits by each types of lightning strokes. Cloud to Ground, Inter Clouds, Intra Clouds and Cloud to Space are few major types of them (See figure 1.2). In addition, there are few minor types were also recognized called Dry lightning, Rocket lightning, Positive lightning, Ball lightning and Upper-atmospheric lightning.

1.2.5 Frequency of occurrence of lightning

The frequency of occurrence of lightning is basically defined as the flashers occurring per unit area per year. Due to the practical difficulties and necessity of very sophisticated equipment the frequency of occurrence of lightning is calculated by an alternative way by using an easily determined parameter called Keraunic level. This Keraunic level is defined as "the number of days in the year on which thunder is heard" [3]. It does not even distinguished between whether lightning was heard only once during the day or whether there was a long thunderstorm. Fortunately, it has been found by experience that the Keraunic level is linearly related to the number of flashers per unit area per year [3].

1.3 Lightning data of Sri Lanka

In 1968, there was a study called "lightning conditions in Ceylon, and measures to reduce damage to electrical equipment" which was carried out by Dr. Gi-ichi Ikeda by an Asian Productivity Project TES/68 [3]. In that study he has compiled the weather

reports from 1931 to 1960 to generate the Isokeraunic Levels (IKL) as shown in the Figure 1.4 [5].

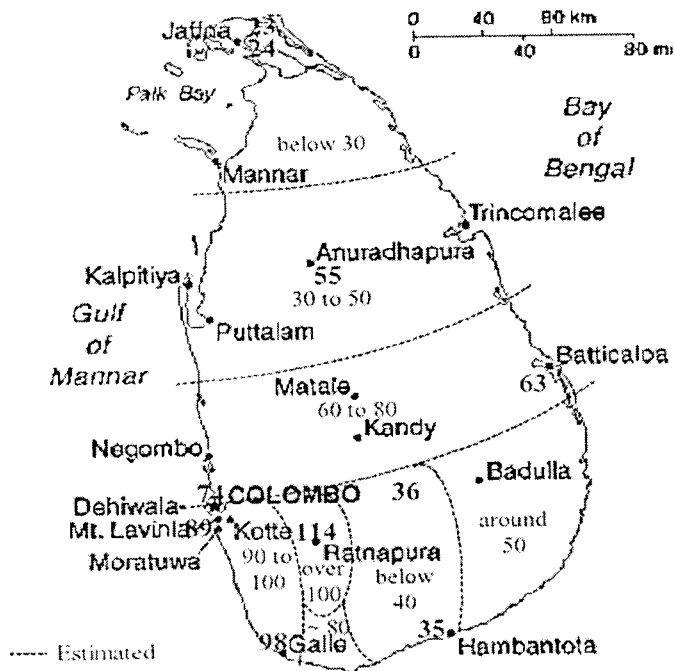


Figure 1.4 – Isokeraunic Level (IKL) map of Sri Lanka [5]

1.4 Introduction to transmission system of Sri Lanka

The power transmission system of Sri Lanka is solely owned and controlled by the Ceylon Electricity Board of Sri Lanka and presently comprises only 132kV and 220kV transmission lines interconnecting grid substations and power stations.

In early 1960s, the 132kV transmission lines were introduced with the development of Laxapana cascaded hydro power complex associated with Kehelgamu-Oya and Maskeli-Oya river basins. Similarly the 220kV transmission lines were introduced to the system in 1980s with the development of Mahaweli Hydro Power complex associated with the Mahaweli river basins. Subsequent developments in the transmission system have expanded the network in to the present state as shown in Annex-1 and Annex-2. Presently there are about 76nos. of transmission lines operating in the network connecting about 75nos. of transmission network points including power stations. The transmission network is presently controlled by the System Controlled Centre located at Dematagoda.

1.5 Lightning effects on power transmission lines

When charged clouds formed above a transmission line, causes to induce positive charges on shield wires as well as on phase conductors due to the negative charges at the bottom of clouds as shown in figure 1.5. This leads to form capacitances between

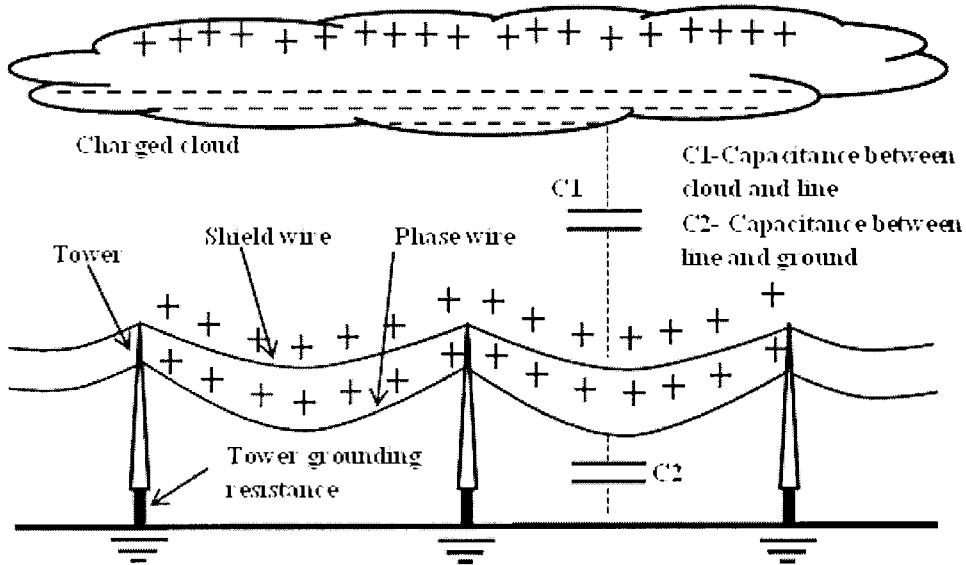


Figure 1.5 – Induced charges on a power transmission line

cloud to line, cloud to ground and line to ground; those will exist until the charge at cloud disappears by a lightning stroke. There are several discharging paths existing for these capacitors depending on the lightning stroke behavior and ultimately causing great damages and line interruptions.

There are three major possibilities of lightning stroke behavior causing line interruptions.

Case 1:

When a lightning leader strokes on to a tower or shield wire will discharges the capacitance between clouds to shield wire. This leads to flow heavy surge currents through towers to ground and casing tower potential rise in association with high grounding impedance of towers. Potential rise in towers induces extremely high stresses across line insulators which lead to flashover from tower to phase/line conductors called back flashovers.

Case 2:

When a lightning leader strokes on to a line/phase conductor (called as shielding failures), will induces very high voltages due to the direct discharge of capacitance between cloud to line/phase conductors. Basically the travelling waves will be generated on the line and causing high voltage stresses across the line insulation leads to breakdown at even low currents. The insulation failure is usually occurs at line insulators at towers whereas flashovers between phase/line conductors at mid spans are very rear.

Case 3:

When a lightning leader strokes to nearby ground directly or through any other grounded object, the capacitance between the cloud and ground will be discharged. Thereby the induced charges at towers and all other conductors will be discharged while forming travelling waves on conductors. In addition there is a possibility of potential rise on towers at close proximity of the lightning struck points due to the ground potential gradients formed by the lightning stroke. Thereby voltages will be appeared across insulators due to those combined actions of travelling waves and potential rise on towers leads to flashovers. Anyhow the flashover incidents of this kind is very rare and not a considerable fact in transmission system voltages higher than 66kV [3].

Parameter	Minimum	Typical	Maximum
Number of return strokes per flash	1	2 to 4	26
Duration of flash (s)	0.03	0.2	2
Time between strokes (ms)	3	40 to 60	100
Peak current per return stroke (kA)	1	10 to 20	250
Charge per flash (C)	1	15 to 20	400
Time to peak current (μ s)	<0.5	1.5 to 2	30
Rate of rise (kA/ μ s)	<1	20	210
Time to half value (μ s)	10	40 to 50	250
Duration of continuing current (ms)	50	150	500
Peak continuing current (A)	30	150	1600
Charge in continuing current (C)	3	25	330

Table 1.1 – Range of values for lightning parameters [6]

1.6 Lightning Parameters

There are several lightning parameters (See Table 1.1) of primary interest to the electric power utility engineer are defined and used to address the lightning issues as described in the previous section. Some of them are described in the following sections.

1.6.1 The quantity of lightning activity in a given area

The quantity of lightning activity is ideally measured in terms of the number of lightning flashes per unit area per year, called the Ground Flash Density (GFD). This value, denoted as N_g , is in units of flashes per km^2 per year. Today, the GFD is usually measured by use of lightning location systems, either by gated wideband magnetic direction-finding systems or time-of-arrival systems. Before using these advanced systems the GFD is calculated with the aid of local IKL data. The IEEE and CIGRE recommend a rough relationship of GFD and local IKL as shown in the equation 1-1 below [6].

$$\text{GFD} = 0.04 T_d^{1.25} = 0.054 T_h^{1.1} \quad (1-1)$$

Where:

GFD = average flashes to earth/ km^2 /year

T_d = average thunder days per year (keraunic level)

T_h = average thunder hours per year (keraunic level)

1.6.2 The distribution of the crest current of a lightning flash

A primary database for lightning parameters was initially developed by Professor Karl Berger in Switzerland based on the number of strokes recorded on 70m and 80m high masts, located on top of the 650m high Mount San Salvatore. There were 1196 flashes in 11 years. Out of these, 75% were negative-upward, 11% were negative-downward, and the remainder was positive-upward [6]. These data was used in combination with some other recorded data at different countries to form the well know CIGRE crest current distribution curve. In addition to the CIGRE distribution cure there was a another equation formulated to obtain the crest current distribution curve by Anderson [6] and adopted by the IEEE/PES Working Group on Estimating the Lightning Performance of Transmission Lines.

Both these curves give almost the same distribution with deviations at very low and very high currents where the available lightning data is minimum (See figure 1.6).

1.6.3 The wave shape of a lightning flash

Almost all lightning strokes are different from each other and therefore no two stroke current wave shapes are exactly alike, and the variations in wave shape are substantial. Most computer programs that calculate line lightning performance assume a straight rising front, a double exponential wave shape, or a CIGRÉ wave shape.

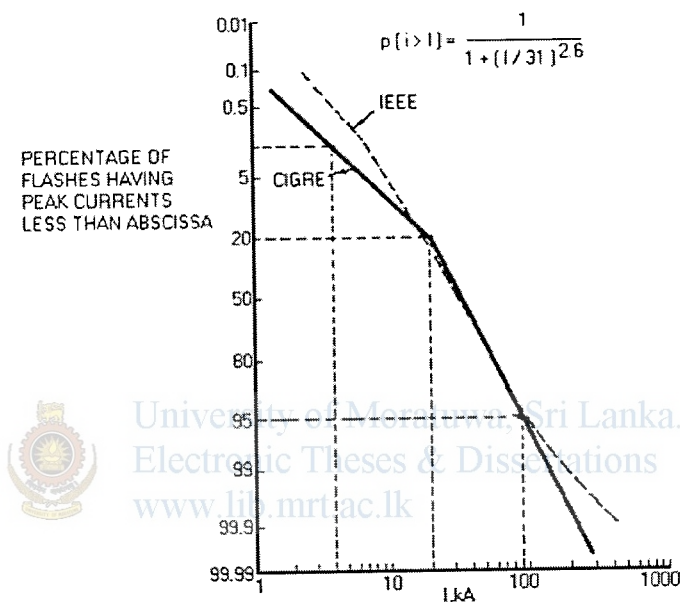


Figure 1.6 – Lightning Stroke Current Probability Distribution [6]

There is no exact rule for the use of a wave shape for EMTP simulations and the selection is depending on the type of EMTP analysis or the application. The front time, tail time, peak current magnitude and the total charge delivered by the stroke current are the basic parameters govern by the wave shape.

1.6.4 Total charge delivered by a lightning stroke

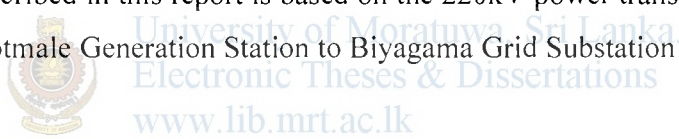
An approximated estimate of total charge delivered by a lightning stroke can be obtained by integrating its current waveform. By this integration results, it clearly shows that higher portion of the total charge delivered is associated with the tail side of the waveform rather at the front of it after the crest current is reached. Therefore the tail time of a lightning current stroke is the governing fact which determines the total charge delivery. Also the total charge in a lightning flash that determines the energy fed into surge arresters, and it is also the charge that causes pitting and burning of

shield wires at contact points. It has been noted that, between some stroke current peaks and at the current decay at the end of lightning flashes, a low, almost direct current, can flow for many milliseconds; more charge can be delivered by this low current than by the high current peaks in a flash. These low currents, because of their longer duration, act somewhat like an arc welder. Continuing currents of hundreds of amperes lasting hundreds of milliseconds have been measured on instrumented towers. These continuing currents can transfer many coulombs of charge in addition to the main portion of the lightning wave shape [6].

Berger [6] integrated the current records of downward flashes to Monte San Salvatore in Switzerland to determine the charges delivered and reported that in one case a positive charge reached 300 coulombs. The positive flashes tend to deliver almost 10 times as much charge as negative flashes, but positive flashes are much less frequent [6].

1.7 Selected transmission line for the study

The case study described in this report is based on the 220kV power transmission line which connects Kotmale Generation Station to Biyagama Grid Substation as shown in the figure 1.7.



This transmission line was commissioned in 1985 as a part of the transmission line project which consists of constructing the 220kV duplex zebra conductor line from

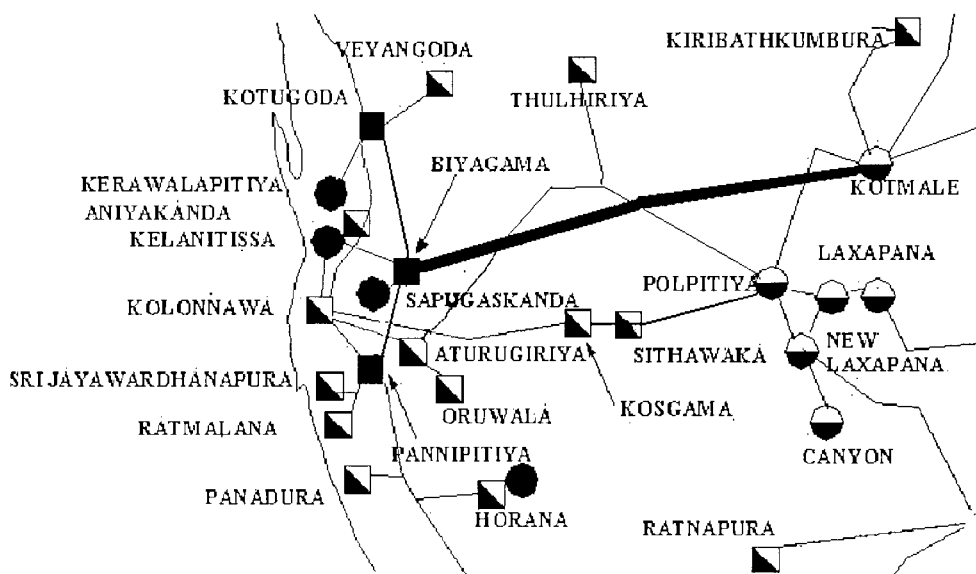


Figure 1.7 – 220kV, Biyagama-Kotmale Transmission Line

Victoria to Biyagama through Kotmale as shown in the figure 1.8.

The transmission line selected in this study is about 70.5km in length and having 206 nos. of double circuit steel lattice towers with 2nos. Galvanized Steel overhead Ground Wires providing protection against lightning. A complete set of line data is attached as Annex 3.

The selected Biyagama-Kotmale 220kV transmission line is one of the critical transmission network elements in the national grid because; this line delivers the highest portion of the generated power from Mahaweli hydro power complex to the loads.

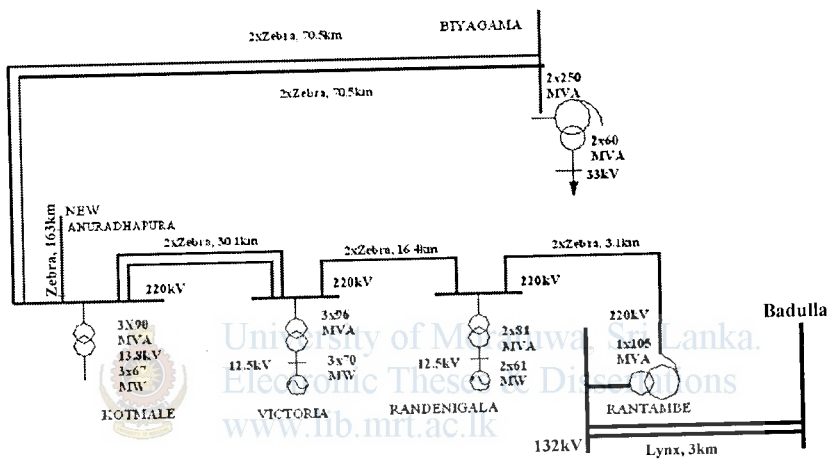


Figure 1.8 – Single line diagram of Victoria complex with Biyagama-Kotmale line

1.7.1 Transmission Towers and configuration

As described in the previous section the selected transmission line consists of 206nos. double circuit, self-standing, steel lattice towers with standard 3m, 6m, 9m and 12m body extensions at some certain locations to maintain the minimum ground clearance value of 7.31m. Therefore the typical tower height will vary between 30 to 35m. Conductor arrangement at towers is in vertical formation where each cross arm holds 02nos. Zebra conductors for each phase. A typical tower drawing is attached as Annex 4.

1.7.2 Insulators and arc horn gaps

Toughen glass Cap & Pin type insulator discs along with galvanized insulator hardware are used to form both suspension and tension insulator strings. Each line insulator string of this transmission line is consists of an arc horn gap where the gap is adjustable at line termination ends only. The gap of arcing horn for a 220kV line is set to be 2m whereas the gap at termination ends will be adjusted as per the insulation coordination requirements of the substation equipment. CEB specification for a single insulator disc is given in Table 1.2.

1.7.3 Phase conductors

Duplex Zebra conductors of 484mm^2 are used for the phase conductors of the selected transmission line having maximum operating temperature at 75°C . As a result the corona performance of the line is better than other available transmission lines due to the increased Geometrical Mean Radius of the conductors. Anyhow the increased corona performance of phase conductors has a negative impact on transient performance due to the reduction of travelling wave-front distortion leads to develop comparatively higher voltages across line insulators.

Dimensions	Units	Suspension string	Tension string
Nominal diameter of disc	mm	254	280
Nominal spacing of disc	mm	146	146
Nominal creepage distance	mm	280	300
Withstand voltages			
Power frequency, Dry	kV	70	70
Power frequency, Wet	kV	40	40
Impulse 1.2x50uS	kV	110	110
Puncture voltage	kV	110	110
Electro mechanical failure load	kN	120	160

Table 1.2 – CEB Specifications for a single insulator disc [4]

1.7.4 Earthing of towers

Earthing of towers is of great importance due to its direct impact on line performance at lightning events. Most of the tower earthing has been done through the tower foundation where a strip of metal bonded to the tower leg is taken out and earth separately. Very low earth resistances in the order of 2Ω to 3Ω are obtained where insitu or precast pile foundations used in marshy soil conditions.

Achieving of CEB specified 10Ω earthing resistance is of great difficulty in the areas where the towers are located in rocky lands or gravel soil conditions. In such cases counterpoise wires were used with specified lengths. Figure 1.9 shows the variation of earthing resistances of selected two line sections having tower numbers 31-52 and 83-97 starting from Kotmale end.

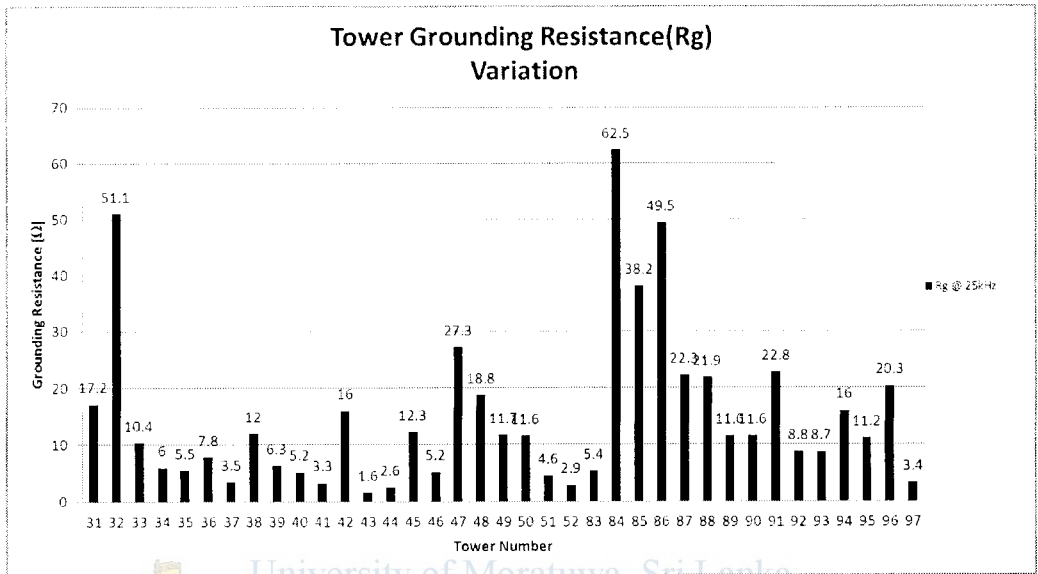


Figure 1.9 – Grounding resistance variation of towers 31-52 and 83-97 starting from Kotmale end



2.1 Introduction

The performance of a power system is mainly depending on the performance of transmission lines. Therefore continues operation of transmission lines without sudden outages is utmost important for the performance in the view point of power delivery as well as system stability. Lightning effects on transmission lines are one of the major reasons which lead to sudden line outages. As described in the section 1.5 of the previous chapter, the back flashover events are the dominant reason of line outages.

The selected 220kV Biyagama-Kotmale transmission line is a double circuit line which delivers the largest amount of power generated by Mahaweli Hydropower Complex to the main load centre at Colombo. Sudden outage of these two circuits creates an excess power generated at Kotmale end and tends to flow through the other two 132kV lines feeding to Badulla and New Anuradhapura Substations connected to Kotmale and Rantembe Substations respectively. Out of these two lines, the new Anuradhapura line has higher impedance due to its higher line length compared to Rantembe-Badulla line. Therefore, Rantembe-Badulla line is more vulnerable to trip off due to overloading. As a result the Kotmale to New Anuradhapura 132kV line will get overload and resulting in loss of all lines connected to the Victoria generation end. Ultimately this creates a sudden loss of around 300MW to the system within few seconds of time which leads the system towards total failure.

Therefore it is utmost important to avoid any double circuit failures by improving the lightning performance of the selected Biyagama- Kotmale transmission line to avoid total failures and associated severe financial losses.

2.2 Preliminary studies

According to the past performance records of this transmission line, it has been noticed that the failure of this transmission line has great influence towards a total failure of the system. Out of those, most of the line outages were due to the effect of

lightning, since most of them were recorded in the months, April to June and October to November where the lightning is frequent.

2.2.1 The relationship between monthly Isokeraunic level and line failures

According to the study [4] it has been found that there is a clear relationship between the monthly Isokeraunic level (IKL) variations with the monthly average failures of this line. Tables and graphs showing the “monthly failures” and “IKL variation with monthly failure variation” respectively are reproduced here including few more recently available data. Table 2.1 shows the monthly line failures from 2004 to 2009 whereas the Figure 2.1 illustrates the relationship of IKL level with the monthly transmission line failures.

Year	January	February	March	April	May	June	July	August	September	October	November	December	Total
IKL [5]	2.5	3.3	7.4	13	7.7	2.2	2.9	2.6	3.7	6.2	6.5	3.3	
2004	0	0	0	0	0	0	0	0	0	1	0	0	01
2005	0	1	0	3	1	3	1	0	0	0	5	0	14
2006	0	0	0	0	0	0	0	0	1	0	0	0	01
2007	0	0	0	0	0	0	0	0	0	0	0	0	00
2008	1	0	0	1	3	2	0	0	0	0	0	0	07
2009	0	0	0	0	3	0	0	0	0	2	2	4	11
Total	1	1	0	4	7	5	1	0	1	3	7	4	34

Table 2.1 – Monthly line failures and IKL

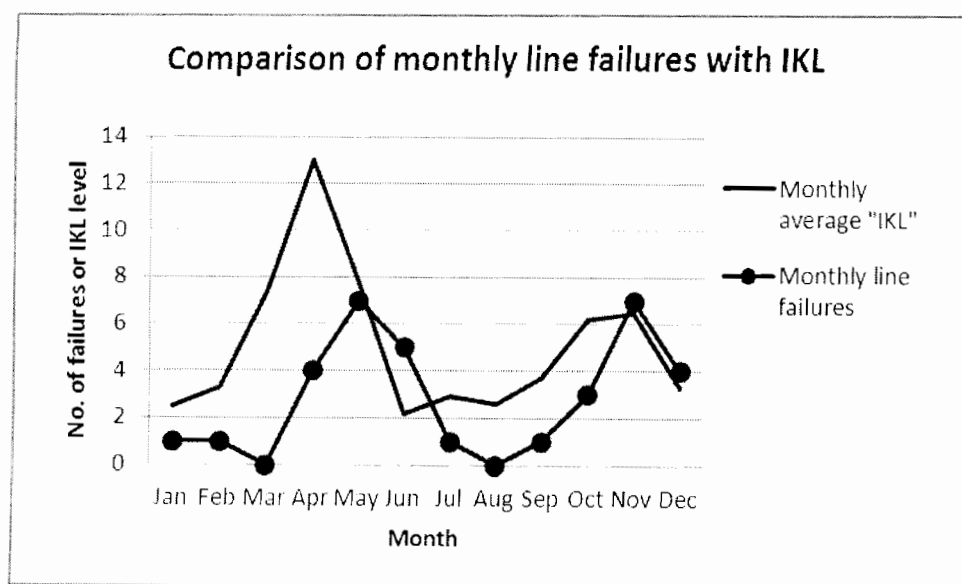


Figure 2.1 – Comparison of monthly line failures with IKL

2.2.2 Line sections having higher probability of insulator failures

It has been found in the previous study [4], that there are two line sections of the selected transmission line have higher probability of insulator damages or flashovers marks according to the breakdown and maintenance records. Those are:

1. The line section having towers, no.33 to 50 and
2. The line section having towers, no.85 to 95 from Kotmale side

Further it has been found that the selected transmission line is crossing over the 132kV Athurugiriya - Polpitiya transmission line at the above two line sections [4]. Therefore the above two line sections have been selected for the study described in this report.

2.3 Back flashover effects on transmission lines

As described in section 1.5, back flashover events occur when the lightning strikes on either tower or shield wires. These strikes produce waves of currents and voltages travelling on the shield wires called travelling waves and reflections occurs at every points where impedance discontinuities. Accordingly surge voltages can be developed across line insulators exceeding the Critical Flashover Voltage (CFO) where flashovers occur from tower to line called back flashovers. The following list shows the parameters those affect the line Back Flashover Rate (BFR).

- a) Ground flash density (See equation 1-1)
- b) Surge impedances of the shield wires and towers
- c) Coupling factors between conductors
- d) Power frequency voltage
- e) Tower and line height
- f) Span length
- g) Insulation strength
- h) Footing resistance and soil composition

According to a previous study [4] the BFR for the selected Biyagama-Kotmale transmission line is calculated as 4.37per year, whereas there is no direct flashover failures can be expected. Therefore it is concluded that the total expected failures are

only due to the back flashover failures of this line which is 4.37per year. Further the calculated expected failure rate 4.37per year is justified by the observed value which is only 4.6per year [4].

2.3.1 Earth faults at power frequency voltage due to back flashover events

An ionization path forms between the Arc horn gaps, when the air insulation between the gaps is breakdown due to a back flashover event. This ionization path acts as a conductive path to form an earth fault condition even at the power frequency voltages. When a transmission line protection system is provided with auto-reclosing facility, the circuit breaker will be reclosed automatically with a set time delay (500ms) after a back flashover trip event to avoid permanent line outage. An earth fault can be developed at power frequency voltage if the ionization path is persists at the moment of first reclosing operation. Therefore the reclosing operation will be blocked and the circuit breaker will be at opened position (breaker lockout) leaving the transmission line at dead condition. This type of line outages can develop severe system instabilities and even total failures. Such events have been reported in the selected Biyagama-Kotmale transmission line in the past history of operation.

Therefore this issue has been addressed in this report by proving a software based analysis approach to provide solutions through a new concept of providing protection called transmission line mounted arresters (TLA).

2.4 Prevention of Back flashover events

Improving tower earthing resistance is the key way of avoiding back flashovers. However it is not practicable as well as not economical when the towers are located at hilly areas where the soil conditions are very bad. Unbalanced or improved line insulation is another way of preventing back flashovers. However this is also not an economical way due to the requirement of additional insulator discs as well as this may need modifications in the towers. Therefore it is found that the most economical and effective way of preventing back flashovers is to install Transmission Line Arresters at selected tower locations.

2.5 Project objectives

The objectives of this study are:

1. Modeling and simulation of 220kV Biyagama-Kotmale power transmission line in EMTP software (PSCAD) for lightning back flashover analysis
2. Conducting sensitivity analysis of line model for back flashover effects
3. Selection and modeling of Transmission Line Arresters (TLA) for EMTP simulations
4. Simulation and performance analysis of line model combined with selected TLAs



University of Moratuwa, Sri Lanka.
Electronic Theses & Dissertations
www.lib.mrt.ac.lk

Chapter - 3

Methodology

3.1 EMTP/PSCAD modeling and simulation

The methodology of analyzing the effects of lightning back flashovers on the selected 220kV Biyagama-Kotmale power transmission line is basically consists of fast front transient modeling and simulation in EMTP type software. The power transmission line and the back flashover event was modeled by frequency dependent fast front transient models due to the nature of higher frequency dependency of lightning strokes typically ranging from 1kHz to 30MHz [1]. Simulation of the model was done for several cases varying some parameters which are highly affecting the back flashover occurrence, to analyze the behavior of power transmission line for such conditions.

EMTP software's are widely used by the most of power utilities to model, analyze and to find solutions for power system transient related problems like lightning effects, GIS switching effects, transient condition analysis of electric machines, harmonic analysis, power quality issues, power electronics and etc. PSCAD is well-known worldwide EMTP software developed by Manitoba HVDC research Centre in Canada, which was conceptualized in 1988 and began its long evolution as a tool to generate data files for the EMTDC simulation program. PSCAD was first introduced as a commercial product as Version 2 targeted for UNIX platforms in 1994 and now available for windows platforms with user friendly interface and highly sophisticated tools and a well-developed simulation engine being fully mature for many years.

The PSCAD was used as the EMTP software in this study for modeling and analyses of lightning back flashover effects on 220kV Biyagama-Kotmale power transmission line. Each of the transmission line elements were modeled by internationally accepted fast front transient models proposed by various studies carried out previously. Some of the elements like transmission line and metal oxide surge arresters were modeled by using the standard library models available in the PSCAD itself. All the other models were selected from various international publications in this field.

3.2 Proposed electromagnetic transient model for 220kV Biyagama-Kotmale transmission line

The basic fast front transient transmission line model which was implemented in the PSCAD is shown in the figure 3.1. The complete line model consists of several sub models representing the following transmission line elements.

- “Transmission line section models” including towers up to the line end terminations (ex: line section with towers from tower no.01 to L1 as shown in the figure 3.1)
- “Transmission line span models” between consecutive towers under study (ex: span between tower no. L1 to M as shown in the figure 3.1)
- Transmission tower model
- Tower grounding resistance model
- Line insulator string with back flashover model
- Line end termination model
- Surge Arrester model
- Lightning surge generator model
- Power frequency phase voltage generator model

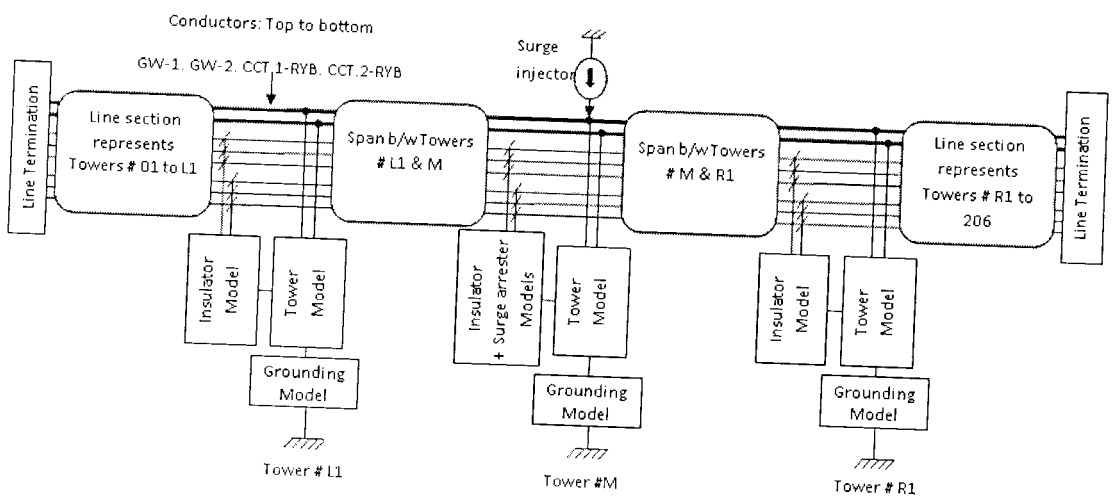


Figure 3.1 – Complete transmission line model proposed for the analysis

As shown in figure 3.1, the complete line model consists of three towers named by tower number M, L1 and R1 represent a typical tower and two adjacent towers at the

left and right sides of it respectively. The two line spans between these three towers were represented by the “line span models” whereas the rest of the line sections at each side up to the end terminations were represented by “line section models”. Six number of inter connecting lines were used to connect each modules while representing the ground and phase conductors from top to bottom sequence as shown in the figure 3.1. The corresponding phase conductor configuration at towers is shown in the Annex 4. All three tower models are connected to the Ground Wire-1(GW-1) and Ground Wire-2 (GW-2) whereas the connections to the phase conductors are made through the insulator models. The surge generator (Current source) is always connected to the top of the middle tower under study.

3.3 Electromagnetic fast front transient sub models for transmission line elements

The sub models used for the implementation of complete EMTP line model is describes in the following sections.

3.3.1 Frequency dependent (Phase) model representing Transmission line sections and spans

The transmission line sections as well as line spans were modeled by using a standard fast front transient module available in the PSCAD library called “Frequency Dependent (Phase) Model” component with different parameter settings to suit both these line elements. This standard model was incorporated in to PSCAD in 1999

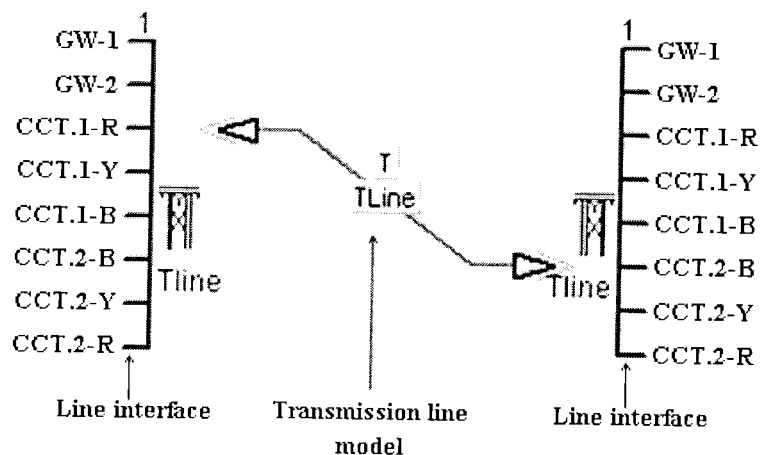


Figure 3.2 – Frequency Dependent (Phase) Model in PSCAD and its connection arrangement

based on the theory proposed in [2]. Basically the Frequency Dependent (Phase) Model is developed based on the distributed RLC travelling wave model while incorporating the frequency dependency of all line parameters by its internal transformation matrices.

The basic parameters those were fed in to the model are attached as Annex 3.

The figure 3.2 shows a typical Frequency Dependent (Phase) Model component available in PSCAD with its connection arrangement. Two standard line interface modeules available in the PSCAD were also used to built up the interconnection between the Phase module to the rest of the system at both sides.

3.3.2 Loss-Less Constant Parameter Distributed Line (CPDL) model representing the transmission towers

The transmission towers were represented by a transient model used in [7], called “Loss-Less, Constant Parameter Distributed Line Model (CPDL)” for Lightning Surge Analysis of transmission Towers. The model was originally proposed in [8].

A transmission tower is represented by a set of series surge impedances each individually represents the tower section between the cross arms as shown in the figure 3.3. The transmission tower is assumed as a loss less vertical transmission line in this study. The surge impedance of a tower is calculated by the formula given in [7,

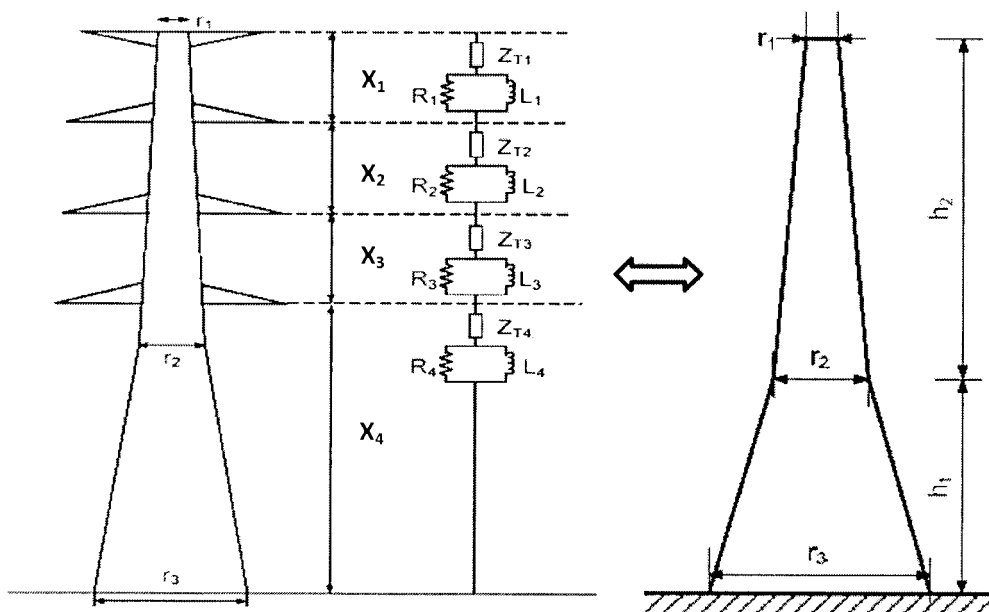


Figure 3.3 – Constant Parameter Distributed Line (CPDL) Model for Towers

9] for “waisted tower shape” as shown in figure 3.3 and recommended by IEEE and CIGRE [10]. The formula is given in the equation 3-1 below. The surge impedances representing each tower sections between cross arms as well as bottom cross arm to ground are assumed to be equivalent to form the CPDL tower model in this study. The cross arms are not represented in the tower model.

$$Z_{T-waist} = 60 \cdot \ln[\cot\{0.5 \cdot \tan^{-1}(R/h)\}] \quad (3-1)$$

Where,

$$R = (r_1 h_2 + r_2 h + r_3 h_1) / h \text{ and } h = h_1 + h_2$$

The frequency dependent effects have to be considered when the surge waves travelling along the towers. Therefore parallel R-L circuits were introduced for each body sections to represent travelling wave attenuation and distortion as shown in the figure 3.3. The propagation wave speed in the tower is assumed to be equal to the Speed of light. The tower travelling time (τ_t) is given by the Equation 3-2.

$$\tau_t = \frac{h}{c} \quad (3-2)$$

Where, h= Tower height and C=Speed of light (300m/ μ s)

The R and L values are determined as a function of Surge Impedance, travel time (τ_t), distances between cross arms (x_1, x_2, x_3 , and x_4) and attenuation factor ($\alpha=0.89$ [7]) as shown in the Equations (3-3) and (3-4) respectively.

$$R_i = \frac{x_i}{h} \cdot 2 \cdot Z_i \cdot \ln\left[\frac{1}{\alpha}\right] \quad (3-3)$$

$$L_i = 2 \cdot \tau_t \cdot R_i \quad (3-4)$$

Where $i=1, 2, 3, 4$

The calculated parameters for a typical tower model are shown in the table 3.1.

#	Parameter	Symbol	Value	Unit
	Tower surge impedance	Z_T	125.7	Ω
	Travelling time	τ_t	0.15	μ s
	Damping resistances	R1	1.96	Ω
		R2	4.05	Ω
		R3	4.10	Ω
		R4	19.20	Ω
	Damping inductances	L1	0.586	μ H
		L2	1.207	μ H
		L3	1.223	μ H

		L4	5.723	μH
Tower data used for calculation:				
	Tower height	h	45	m
	Equivalent radius (See figure 3.3)	r ₁ , r ₂ , r ₃	1.55, 2.85, 11.91	m
	Cross arm distances(See figure 3.3)	x ₁ , x ₂ , x ₃ , x ₄	3.00, 6.18, 6.26, 29.3	m

Table 3.1 – Calculated parameters for a typical tower model

3.3.3 Tower grounding resistance model

The tower grounding resistance is not a constant for a fast front surges and it varies as per the surge current magnitude. This is due to the soil ionization and breakdown characteristics of the soil surrounding the tower grounding electrodes. At certain surge current magnitudes create voltage gradients sufficient to breakdown the soil and forms conductive paths to flow the current, ultimately reduces the grounding resistance. Therefore the impulse grounding resistance is less than the grounding resistance values measured at low current and low frequency states. The relationship between impulse and non-impulse grounding resistances can be expressed as in Equation 3-5.

$$R_f = R_g / \sqrt{1 + \{I/I_g\}} \tag{3-5}$$

Where,

R_f is the impulse tower grounding resistance (Ω)

R_g is the tower grounding resistance at low current and low frequency (Ω)

I is the surge current in to ground (kA)

I_g is the limiting current initiating soil ionization (kA) as given in the Equation 3-6

$$I_g = \frac{1}{2\pi} \frac{E_o \rho_o}{R_g^2} \tag{3-6}$$

Where,

ρ_o is the soil resistivity (Ωm)

E_o is the soil ionization gradient (about 300kV/m)

The variation of impulse grounding resistance (R_f) of towers 31 to 52 and 83 to 97 for surge currents from 30kA to 200kA with 10kA step was calculated and graphed as shown in the Annex 6. It was observed that the variation is raging from maximum 17.2 Ω to minimum 1.6 Ω for the surge currents from 30kA to 200kA.

Therefore the grounding resistance values can exist higher than the CEB specified value (which is the 10Ω) even with the soil ionization effect.

Therefore the grounding resistance of a tower is represented as a variable resistance in the EMTP (PSCAD) model which changes its value from 10Ω to 100Ω with 10Ω steps.

3.3.4 Line insulators and back flashover model

The line insulator strings between tower and phase conductors are represented as a capacitor in the EMTP (PSCAD) model. Each high voltage glass insulator disc has a capacitance in the range of 30pF to 40pF. An equivalent capacitance of 2.8pF is used for an insulator string having 17 nos. of insulator discs.

The transient-voltage withstand capability of an insulator string with an arc horn gap is vary with the time of which it is under voltage stress. An insulator string can withstand very high transient-voltages for shorter time duration whereas it may breakdown by a comparatively low transient-voltage if applied for a longer duration. This characteristic of an insulator string is known as the volt-time characteristic or in another term called flashover characteristics. This characteristic variation of flashover voltage of an insulator string can be modeled by a simplified expression given in the Equation 3-7.

$$V_{fo} = K_1 + \frac{K_2}{t^{0.75}} \quad (3-7)$$

Where,

V_{fo} is the flashover voltage (kV)

$$K_1 = 400 \times A_g$$

$$K_2 = 710 \times A_g$$

A_g is the Arc-horn gap length (m)

t is the elapsed time after lightning stroke (μ s)

Flashover voltage-time characteristic of 220kV line insulator string having 2m Arc-horn gap is shown in the Figure 3.4.

The back flashover event occurs when the transient voltage developed across the insulator string is greater than its withstanding voltage (Flashover voltage - V_{fo}). Once

the back flashover mechanism is triggered the voltage across the insulator string will be collapsed to zero by creating conductive path through the air insulation. Therefore back flash over event is modeled by a Circuit Breaker used as a switch, placed parallel

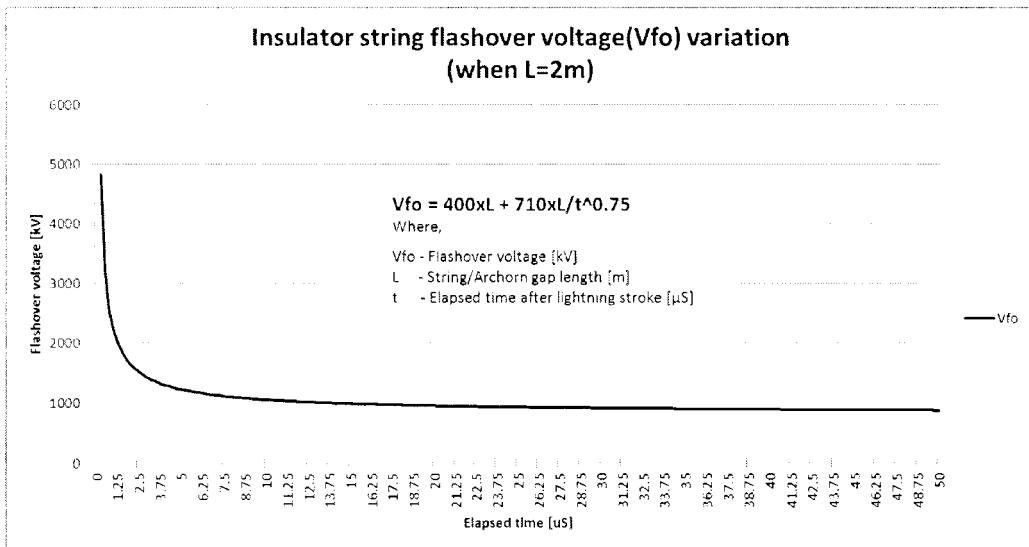


Figure 3.4 – Flashover voltage-time characteristic of 220kV line insulation with 2m Arc-horn gap

to the equivalent capacitance of insulator string. The close-operation of the Circuit Breaker (in this case closing the switch) is controlled by an external control module as shown in the Figure 3.5. www.lib.mrt.ac.lk

The external control module compares the voltages developed across the insulator string with its volt-time characteristics. If the developed voltage profile crosses the

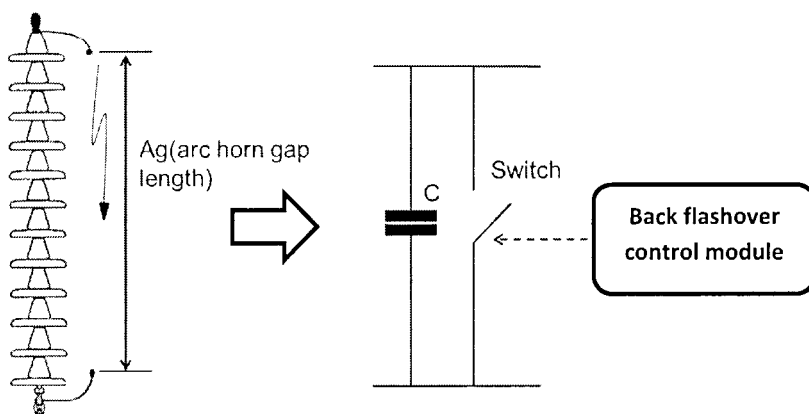


Figure 3.5 – Insulator string and back flashover model

flashover volt-time characteristics of insulators, the control module closes the circuit breaker to create a back flashover event. The back flashover control module is developed by using the standard control components available in the PSCAD.

The line insulator string voltage and line voltage are used as the basic input parameters to generate the elapsed time as shown in the Figure 3.6. Generated elapsed

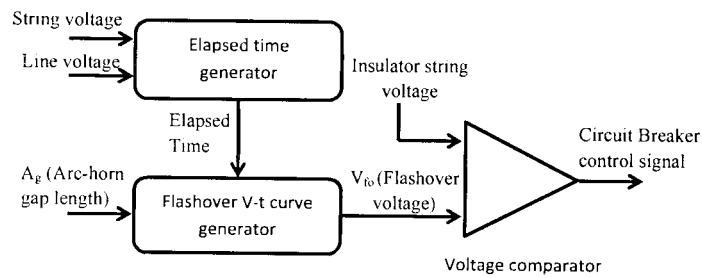


Figure 3.6 – Basic logic diagram for back flashover control module

time and Arc-horn gap length are taken as inputs to Flashover V-t curve generator module to produce the flashover voltage. Finally the voltage comparator module compares the insulator string voltage with generated flashover voltage and issues the Circuit Breaker close signal if a back flashover voltage is present.

3.3.5 Line termination model

The two ends of transmission line model were grounded through equivalent surge impedances of the line and ground conductors to avoid end reflections. An equivalent

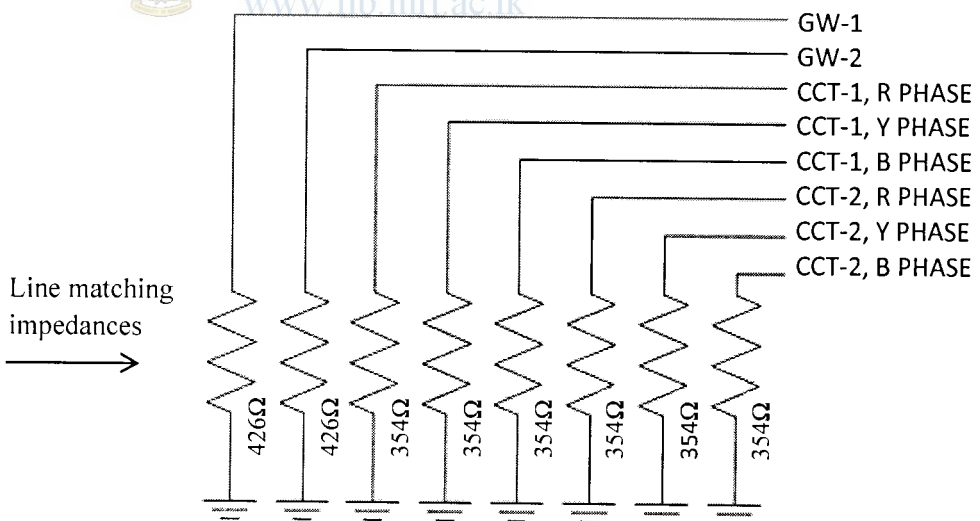


Figure 3.7 – Grounding arrangement of a typical end termination model

impedance of 354Ω for phase conductors and 426Ω for ground conductors were used at both ends [4]. The grounding arrangement of a typical end termination model is shown in the Figure 3.7.

3.3.6 Surge arrester model

ABB made, gapless type, Metal Oxide Transmission Line Arrester (TLA) is used in this study as a solution for the back flashovers and its related issues. The selected TLA is represented by a fast front surge arrester model described in [11] which is a modified version of the model proposed in [12].

The arrester model consists of two nonlinear resistors designated as A_0 and A_1 , representing the V-I nonlinear characteristic of the arrester as shown in the Figure 3.8.

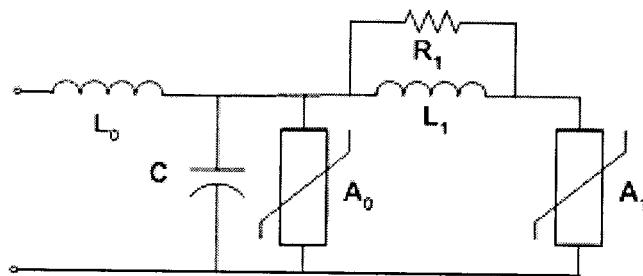


Figure 3.8 – Frequency dependent surge arrester model

Two nonlinear resistors are separated by an R-L filter. For slow front surges (e.g. switching surges), the R-L filter has very low impedance and the two nonlinear resistances acts as parallel. For fast front surges, (e.g. lightning surges) the impedance of the R-L filter becomes significant and as a result more current flows in the nonlinear resistor A_0 than in A_1 . As shown in the Figure 3.9 the A_0 has a higher voltage characteristic than A_1 for a given surge current. Therefore higher discharge voltages are developed across arrester model for fast front surges. Since metal oxide arresters have a higher discharge voltage for fast front surges, the model matches the overall behavior of a metal oxide arrester [12].

The inductance L_0 represents the inductance from the magnetic fields in the immediate vicinity of the arrester. The capacitance C represents the terminal-to-terminal capacitance of the arrester [12].

The RLC elements of the arrester model are initially determined by the following formulas given in [12].

$$L_1 = 15d/n \text{ (}\mu\text{H)} \quad (3-8)$$

$$R_1 = 65d/n \text{ (}\Omega\text{)} \quad (3-9)$$

$$L_0 = 0.2d/n \text{ (}\mu\text{H)} \quad (3-10)$$

$$C = 100n/d \text{ (pF)} \quad (3-11)$$

Where,

d = the estimated height of the arrester in meters (uses the overall dimension from the catalog data of selected arrester)

n = number of parallel columns of metal oxide in the arrester

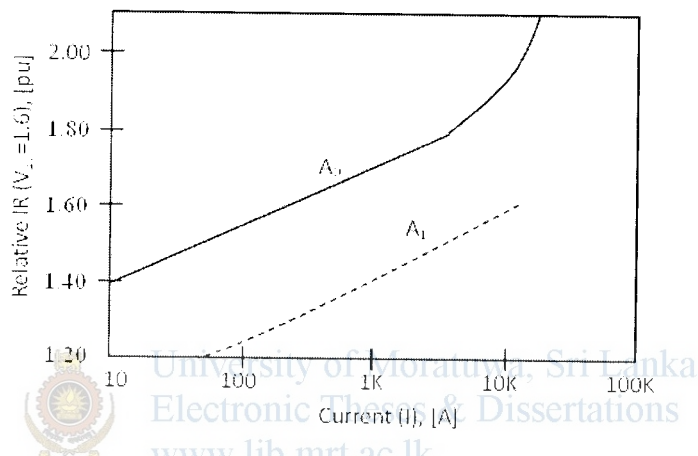


Figure 3.9 – V-I Relationship for nonlinear resistors A_0 and A_1 [12]

The nonlinear resistors A_0 and A_1 can be modeled in the EMTP as a piecewise linear V-I curve with characteristics defined point by point [12]. The initial, individual nonlinear characteristics of A_0 and A_1 are determined based on the graph produced in the Figure 3.9. Each of the V-I points for the nonlinear resistors is found by selecting a current point and then reading the relative IR in pu from the graph. This value is then multiplied by $(V_{10}/1.6)$ to determine the model discharge voltage in kV for the associated current. (V_{10} is the discharge voltage for a 10kA, $8 \times 20 \mu\text{s}$ current in kV) This scaling from pu to actual voltage is done by the application of the following formula to the "Relative IR" pu voltage found for that current as given in Figure 3.9 [12]. For A_0 the

$$\text{Discharge kV} = [\text{Relative IR in pu for } A_0(i)] \times [V_{10}/1.6] \quad (3-12)$$

Likewise for A_1 , the

$$\text{Discharge kV} = [\text{Relative IR in pu for } A_1(i)] \times [V_{10}/1.6] \quad (3-13)$$

3.3.7 Lightning stroke current generator model

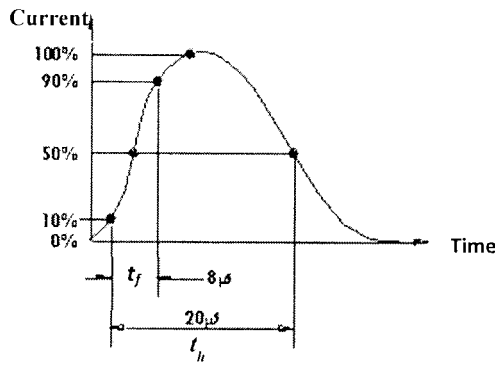
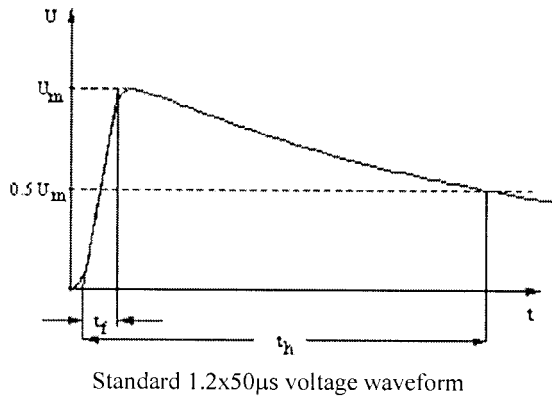
A lightning strike generally consists of several return strokes, where the average number of strokes in a lightning strike is roughly about three. According to the statistics of return strokes peak current distribution, one can assume that the first return stroke in a lightning strike is at least severe as subsequent strokes. Therefore the latter can be ignored [6]. Therefore in lightning transient studies, it is considered only the first return stroke.

The characteristics of real lightning current wave shapes are determined by its polarity, maximum instantaneous value, steepness and equivalent front/tail times. The maximum instantaneous value (peak current) is statistically related to the steepness or time to crest of the current waveform. The steepness increases as the peak current increases.

The lightning stroke is modeled by a current source which produces the standard double exponential (see Equation 3-14) current waveform $8 \times 20 \mu\text{s}$ of positive polarity with variable peak current as shown in the figure 3.10.

In addition to the $8 \times 20 \mu\text{s}$ current waveform; standard $1.2 \times 50 \mu\text{s}$ voltage waveform was also used separately for the simulations. (See figure 3.10)

The same double exponential waveform was used with relevant α and β values to generate the $1.2 \times 50 \mu\text{s}$ lightning surge waveform.



University of Moratuwa, Sri Lanka.
Electronic Theses & Dissertations

U_m = Peak magnitude

t_f = Wave front time (Time to reach current magnitude from 10% U_m to 90% U_m)

t_h = Wave tail time (time to drop magnitude from peak to 50% U_m)

Figure 3.10 – Standard waveforms for lightning surge voltage and current

$$I(t) = I_o (e^{-\alpha t} - e^{-\beta t}) \tag{3-14}$$

Where,

$I(t)$ = lightning current

I_o = Peak current magnitude

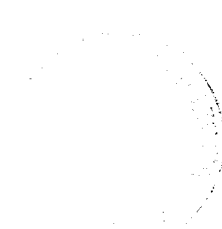
$\alpha = 8.66 \times 10^4 \text{ s}^{-1}$ for 8x20µs waveform [11]

$\beta = 1.732 \times 10^5 \text{ s}^{-1}$ for 8x20µs waveform [11]

$\alpha = 1.426 \times 10^4 \text{ s}^{-1}$ for 1.2x50µs waveform [3]

$\beta = 4.877 \times 10^6 \text{ s}^{-1}$ for 1.2x50µs waveform [3]

t = time(s)



3.3.8 Power frequency phase voltage generator model

Instantaneous power frequency voltages of each phase were generated by using the following equations.

$$V_a = V_p \sin(\theta) \quad (3-15)$$

$$V_b = V_p \sin(\theta - 120) \quad (3-16)$$

$$V_c = V_p \sin(\theta + 120) \quad (3-17)$$

Where,

V_a , V_b and V_c are the instantaneous phase voltages in kV

θ = the phase angle in radians

$$V_p = 220 \times \sqrt{2/3} = 179.63 \text{ kV} \quad (3-18)$$

Where,

V_p = peak value of phase voltage in kV

Generated power frequency phase voltages are taken as input data to calculate the actual insulator string voltage given to the voltage comparator as shown in the Figure 3.6.



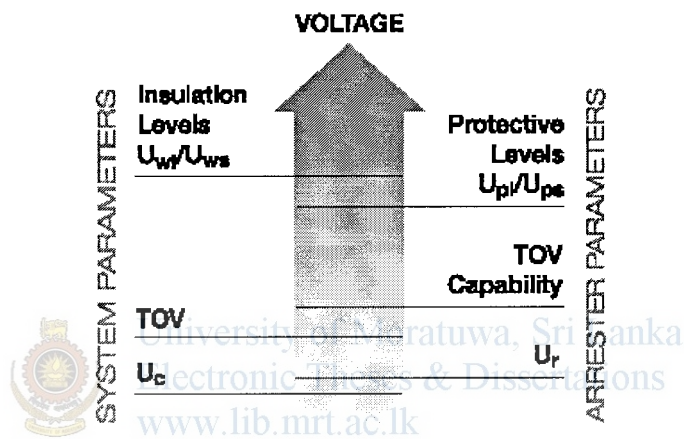
University of Moratuwa, Sri Lanka.
Electronic Theses & Dissertations
www.lib.mrt.ac.lk

3.4 Selection of a Transmission Line Arrester (TLA)

Selection of an ABB transmission line arrester is carried out in two major steps as follows [13].

Step 1: Matching the electrical characteristics of the arresters to the system's electrical demands

Step 2: Matching the mechanical characteristics of the arresters to the system's mechanical and environmental requirements



Vocabulary

U_m	Maximum system voltage	k	Earth fault factor
U_c	Continuous operating voltage	U_{ps}	Switching impulse protective level
U_l	Rated voltage	U_{pl}	Lightning impulse protective level
TOV	Temporary overvoltage	U_{ws}	Switching impulse withstand level
T	TOV strength factor	U_{wl}	Lightning impulse withstand level

Figure 3.11 – System and Arrester parameter matching configuration [13]

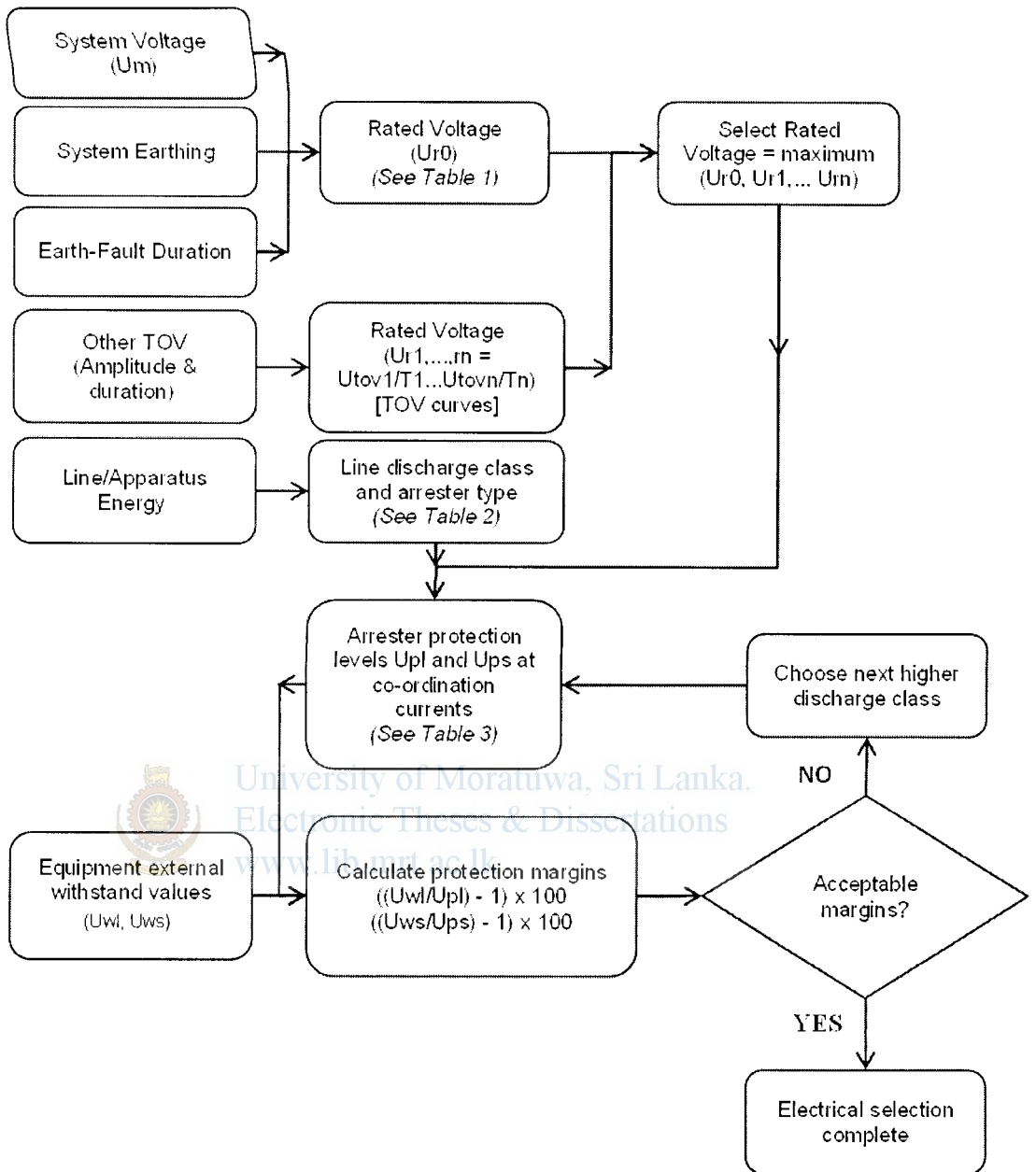


Figure 3.12 – Selection procedure of electrical parameters for ABB surge arresters [13]

In this study, initially only the electrical parameters of the arrester are necessary for the purpose of modeling it in the PSCAD. Therefore only the electrical parameters were selected and match with the system parameters at this stage. Figure 3.11 shows the arrester and system electrical parameter matching configuration as specified in [13]. Step by step selection of an ABB surge arrester as per the selection procedure shown in the Figure 3.12 is given in the Annex 7. Selection and matching of the mechanical parameters has to be done to complete the overall selection procedure and to fulfill the typical installation requirements.

Application of the methodology

4.1 Introduction

This chapter describes the way of implementation of transient modeling concepts which were described in the previous chapter. The implementation of the transient model concepts were carried out in the PSCAD software as a digital model. Further this chapter describes the way of simulation of implemented transient model with the aid of inbuilt “Multiple Run” component which provides effective means of simulation.

4.2 Power Systems CAD (PSCAD) modeling tool

PSCAD (Power Systems CAD) is a well-developed software program which act as a Graphical User Interphase (GUI) to the world renowned electromagnetic transient solution engine called EMTDC (EMTDC stands for Electromagnetic Transients including DC). PSCAD facilitates the users to create models or circuits, simulate them and to analyze the results in a completely integrated graphical environment. Drag and drop type sophisticated Input-Output modules such as meters, controllers, plotters and graphs are available which can even control while the circuits are at simulation run mode. Therefore online control of circuit or model parameters and monitoring of results can be done easily.

PSCAD comes complete with a library of pre-programmed and tested models, ranging from simple passive elements and control functions, to more complex models, such as electric machines, FACTS devices, transmission lines and cables. If a particular model does not exist, PSCAD provides the flexibility of building custom models, either by assembling those graphically using existing models, or by utilizing an intuitively designed Design Editor.

4.2.1 PSCAD Graphical User Interface (GUI) window

PSCAD software comes with a user friendly GUI (Graphical User Interface) which provides an active environment for users to develop solutions by graphical means. The Figure 4.1 shows a typical GUI window of PSCAD software. The GUI can be

divided in to four basic working areas called Workspace Window, Output Window, Design Editor and the rest of the area consists of tool bars, menus and palettes.

The Workspace Window is the central project database for PSCAD which gives an overview of currently loaded projects (i.e. project tree), master library, data files, signals, controls, transmission lines, cable objects, display devices and etc. Further it

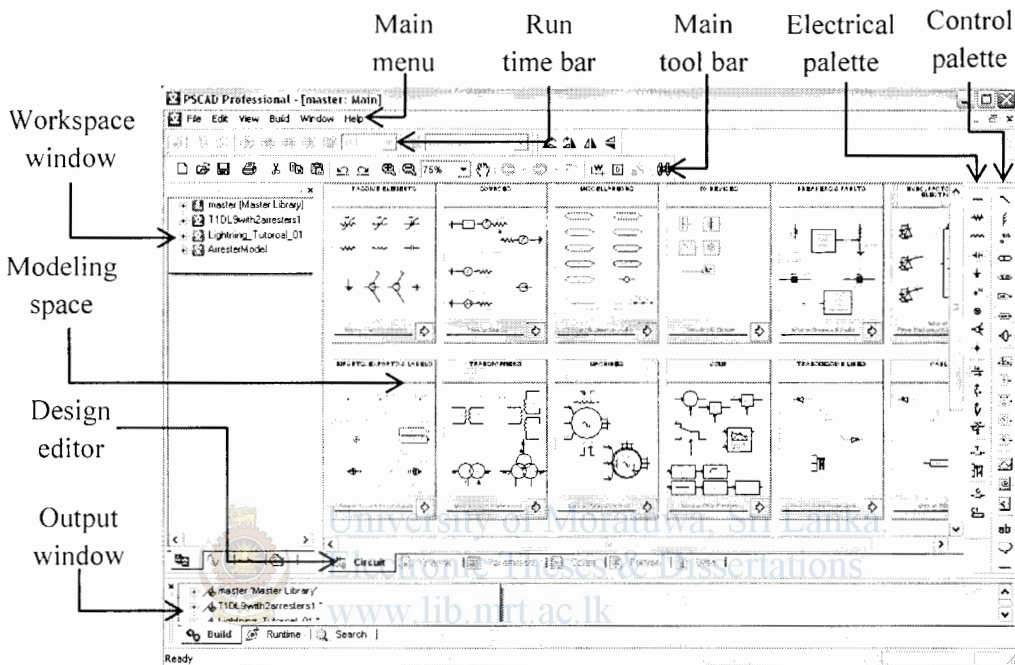


Figure 4.1 – Typical working window of PSCAD software

provides the facility to organize them within the workspace window by drag and drop feature.

The Output Window section provides an easily accessible interface for viewing feedback and troubleshooting of simulations. All the error and warning messages either given by a component, PSCAD or EMTDC can be viewed from the output window section and also provides the facility to locate the errors by double clicking on the error messages.

The Design Editor window is probably the most important part of the PSCAD environment, and is where most (if not all) project design work is performed. The Design Editor is used mostly for the graphical construction of circuits (Circuit view), and also includes an embedded component definition editor.

4.3 Creation of sub models in PSCAD

Following sections describe the sub models which were developed in PSCAD based on the transient model concepts provided in the previous chapter.

4.3.1 Transmission line model

As described in the previous chapter the transmission line sections and line spans were modeled by using the standard frequency dependent phase model available in the Master Library of the PSCAD. There are two basic ways of constructing a

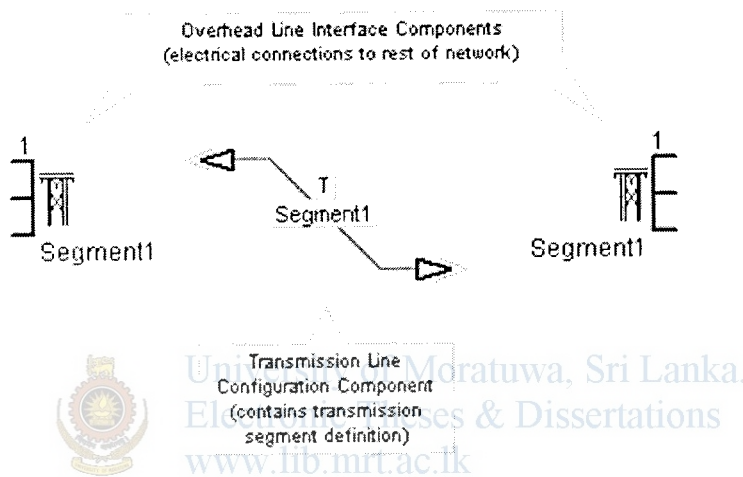


Figure 4.2 – Transmission line model (Remote end method)

transmission line in PSACD by using the above standard model and in this study the remote end method was used (See the Figure 4.2). Creating the transmission line with two line interfacing end components having the same line name is called remote end

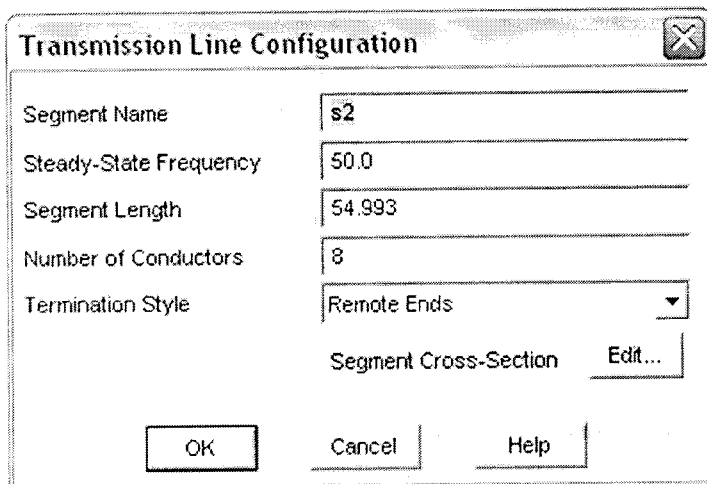


Figure 4.3 – Transmission line parameter input window

method. Conductor configuration of interfacing components is shown in the Figure 3.2.

Transmission line component's parameters were entered in the pop-up window as shown in the Figure 4.3. Selection of "Edit" button in front of the "Segment Cross-Section" as shown in the Figure 4.3 enables the user to enter the parameter values

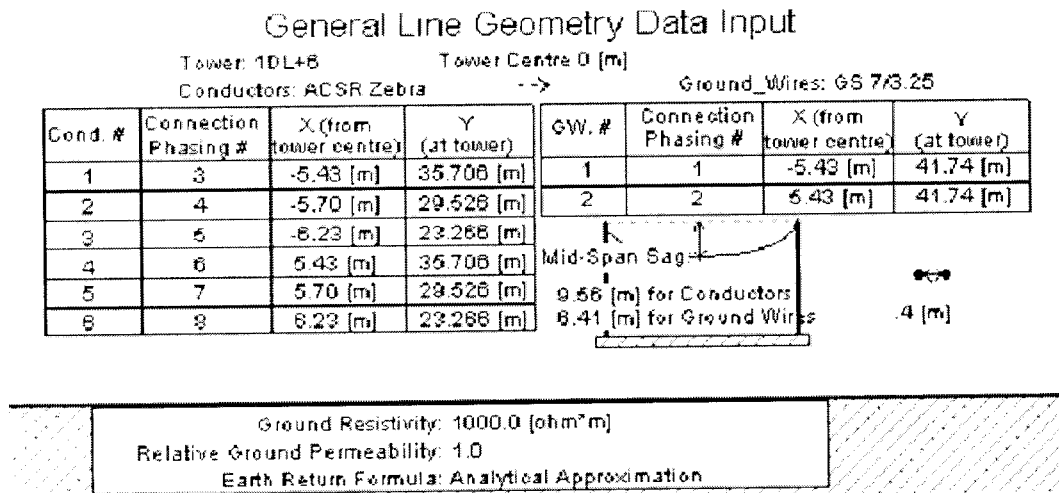


Figure 4.4 – General Line Geometry Data input

(geometrical and electrical properties as attached in Annex 3) of the towers, conductors and ground. A typical geometrical input data set which was fed in to the PSCAD is shown in the Figure 4.4.

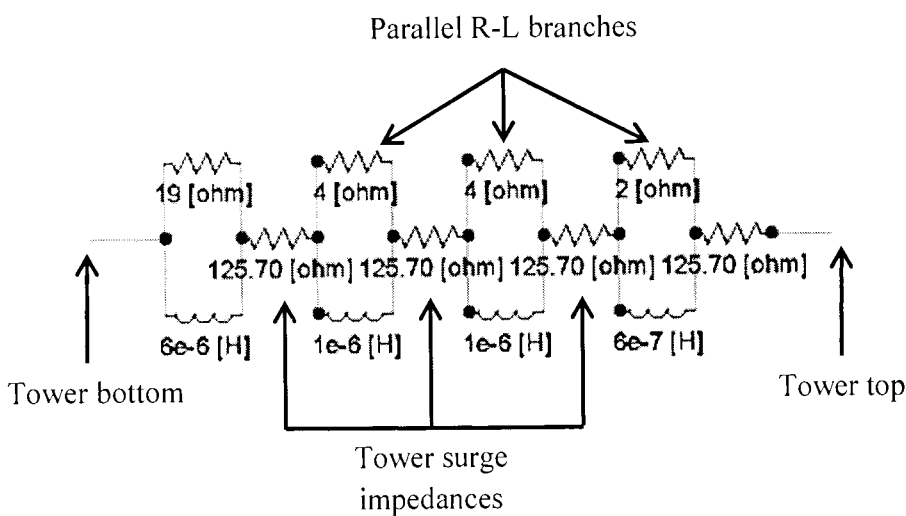


Figure 4.5 – Typical tower model created in PSCAD

4.3.2 Transmission tower model

As per the proposed model in the previous chapter, the transmission towers were model by the Constant Parameter Distributed Line (CPDL) model which consists of four (04) numbers of impedances series with four numbers of parallel Resistance-Inductance branches as shown in the Figure 4.5.

The tower model is created completely by using two basic passive components named resistor and inductor available in the Master Library of the PSCAD. Parameter values of each resistors and inductors were set as shown in the Table 3.1.

4.3.3 Tower grounding resistance model

A variable resistance component available in the PSCAD Master Library is used to

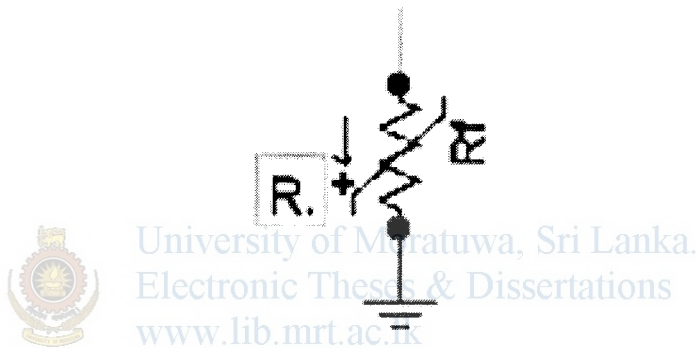


Figure 4.6 – Tower grounding resistance model

represent the Impulse grounding resistance of a transmission tower. The value of the variable resistance was varied externally from 10Ω to 100Ω in 10Ω steps by the “Multiple Run” simulation component as described in the section 4.5. Figure 4.6

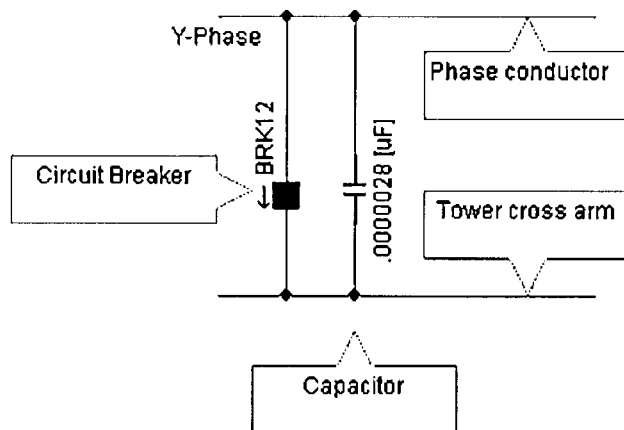


Figure 4.7 – Insulator string capacitor and Back flashover Breaker models

shows a typical impulse grounding resistance model of a tower which was created by the aid of a variable resistor component in PSCAD.

4.3.4 Line insulator string with back flashover model

The insulator string and the back flashover event were modeled by an equivalent capacitor parallel with an externally controlled circuit breaker as shown in the Figure 4.7. As described in the section 3.3.4 in the previous chapter, the operation of circuit breaker is controlled by a back flashover control module shown in the Figure 3.6. The basic logic diagram shown in the Figure 3.6 was implemented in PSCAD (See Figure 4.8) by using basic Control Blocks available in the Master Library.

Insulator String Voltage (Vs11), Line to Ground Voltage (V11), Arc Horn Gap length (=2m) and Instantaneous Phase Voltage (Va) are taken as the input data for the above module. Inbuilt Voltmeter components and their output signals are used to read the Insulator String Voltage (Vs11) and Line to Ground Voltage (V11), whereas the Instantaneous Phase Voltages are given by the Power Frequency Phase Voltage

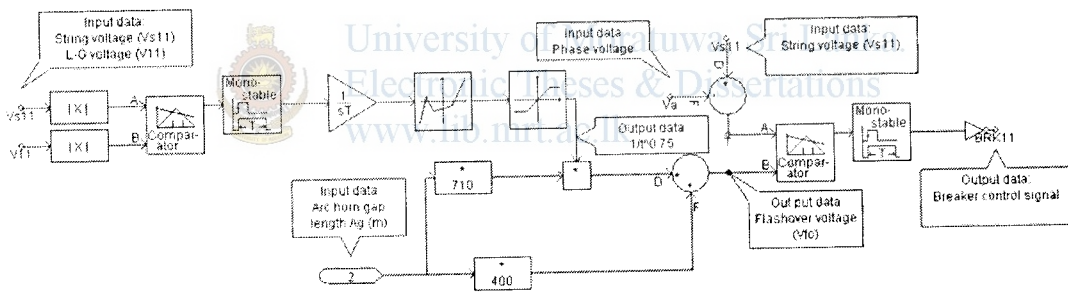


Figure 4.8 – Back flashover control module implemented in PSCAD

Generator model described in the section 3.3.8.

Control components forming the left most branch of the module as shown in the figure 4.8, is calculating the $\frac{1}{t^{0.75}}$ value (t=elapsed time) based on the input data Vs11 and V11. The control components forming the loop, generates the flashover voltage value (Vfo) taking the arc horn gap length (Ag=2m) and the $\frac{1}{t^{0.75}}$ value as the input parameters. The actual insulator string voltage is generated by the upper most Differencing Junction component taking the relevant power frequency phase voltage value and the measured string voltage as input data. Finally the comparator component compares the generated Vfo and actual string voltage values and gives the

output signal as a positive pulse whenever the voltage profiles are crosses each other which formulate a back flashover event. Mono-stable component at the right most side of the model generates a digital output value “1” based on positive pulse generated by the comparator component. Invertor component at the end of the model generate the opposite digital value “0” required as an input data to the relevant Circuit Breaker to close the circuit. Close operation of the circuit breaker creates an external conductive path across the insulator string which simulates the back flashover arc generated across the arc horn gaps.

4.3.5 Power frequency phase voltage generator model

As described in the section 3.3.8, instantaneous power frequency phase voltages were

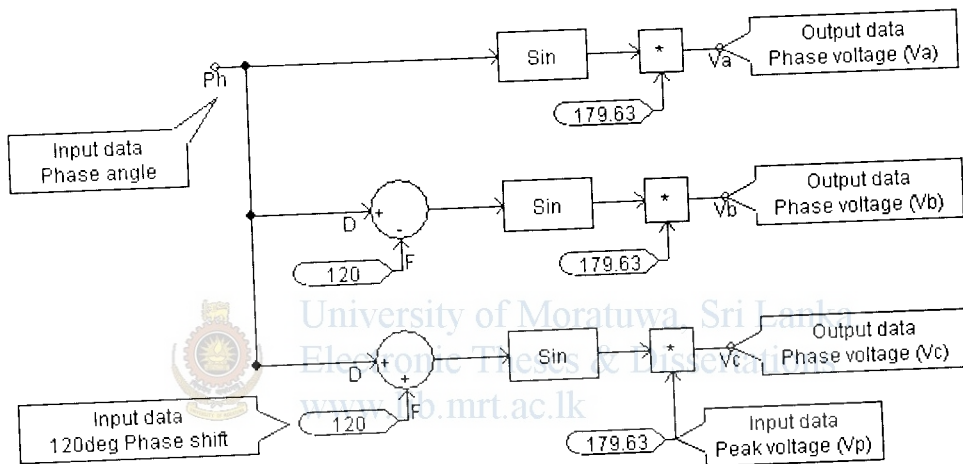


Figure 4.9 – Power frequency phase voltage generator model

generated by using the circuit created in PSCAD (See the Figure 4.9). The circuit is created by modeling the equations 3-15, 3-16 and 3-17 given for each phase voltage variation. Basic control components such as Summing/Differencing junctions, Real/Integer constants, Trigonometric Sin function and multipliers were used to create the circuit as shown in the Figure 4.9. The “phase angle” input data values are given by the “Multiple Run” simulation component as described in the section 4.5.

Output phase voltages, V_a , V_b and V_c were directly used in the back flashover control modules to generate the actual insulator string voltages.

4.3.6 Line end termination model

Two ends of the transmission line were grounded through equivalent surge

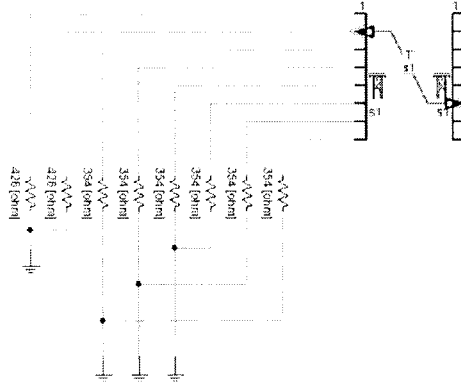


Figure 4.10 – Line termination model created in PSCAD

impedances of each ground and phase conductors as shown in the Figure 4.10. Each end of the grounded impedances was connected to the nearest interfacing component of the transmission line section as per the relevant connection arrangement. Top two terminals of the interfacing component stand for the two Ground Wires and the rest six terminals stand for the phase conductors of each circuit. Phase conductors of both circuits were grounded through 354Ω equivalent impedances and similarly the ground conductors were grounded through 426Ω equivalent impedances.

4.3.7 Surge Arrester model

Construction of surge arrester model in PSCAD is done through the following steps described in [11].

Step 1:

Determination of initial parameter values for L_0 , C , L_1 and R_1 when estimated height of the arrester (d) = 2.105m (for PEXLIM Q type ABB arrester [13]) and number of parallel columns of metal oxide in the arrester (n) = 1.

Calculated initial parameters: (See Figure 4.11)

$$L_1 = 15 \cdot d/n = 15 \cdot 2.105/1 = 31.575 \mu\text{H}$$

$$R_1 = 65 \cdot d/n = 65 \cdot 2.105/1 = 136.825 \Omega$$

$$L_0 = 0.2 \cdot d/n = 0.2 \cdot 2.105/1 = 0.421 \mu\text{H}$$

$$C_0 = 100 \cdot n/d = 100 \cdot 1/2.105 = 47.506 \text{ pF}$$

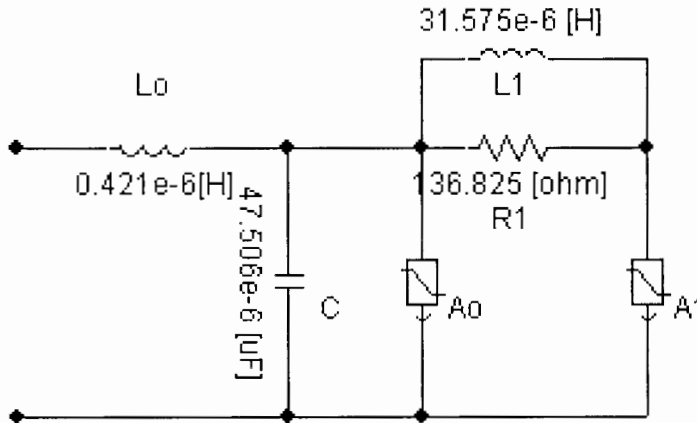


Figure 4.11 – Surge arrester model created in PSCAD

Step 2:

Evaluation of scaling factor $U_{10}/1.6$, to apply to the surge arrester components of both A_0 and A_1 sections under Arrester Voltage Rating in PSCAD

From table-2 in Annex 7, for selected PEXLIM Q type ABB arrester,

U_{10} (Discharge voltage at 10kA) = 423kV

Therefore the Arrester Voltage Rating = $423/1.6 \text{ kV} = 264 \text{ kV}$

Step 3:

Defining of “I-V Characteristic” for both A_0 and A_1 sections and entered into the surge arrester components

Initial I, V values for A_0 and A_1 were set as shown in the Table 4.1.

X-axis current[kA]	A_0 Y-axis voltage [pu]	A_1 Y-axis voltage [pu]
1.0E-7	1.10	0.72
1.0E-6	1.28	1.00
1.0E-5	1.33	1.08
1.0E-4	1.37	1.11

0.001	1.39	1.15
0.01	1.42	1.18
0.1	1.52	1.22
1.0	1.65	1.32
3.816	1.75	1.40
10.0	1.90	1.55
100.0	3.80	1.95

Table 4.1 – Initial I, V values for A_0 and A_1 [11]

Step 4:

Adjustment of the $(U_{10}/1.6)$ scaling factor for the A_1 non-linear resistance section, to match the switching surge discharge voltage. This is done by trial and error until there is a good match between the manufacturers' switching surge discharge voltage U_{ss} and current and the model test results.

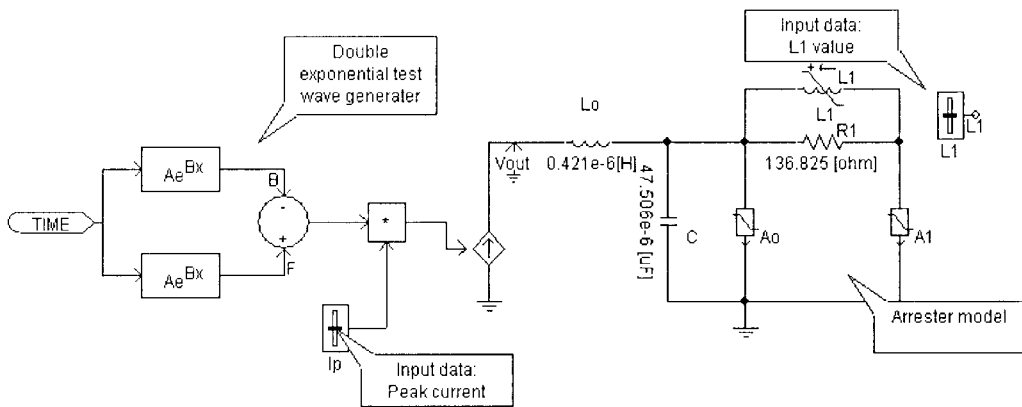


Figure 4.12 – Created test circuit in PSCAD for surge arrester testing

As per the manufactures' data shown in table 2 of Annex 7,

$U_{ss} = 357\text{kV}$ (peak) for 1kA surge of 30/60 μs wave shape.

Therefore a double exponential waveform of 30/60 μ s with 1kA peak current (See Figure 4.13) was generated and applied to the arrester model. Created test circuit in PSCAD for the testing of arrester is shown in the Figure 4.12.

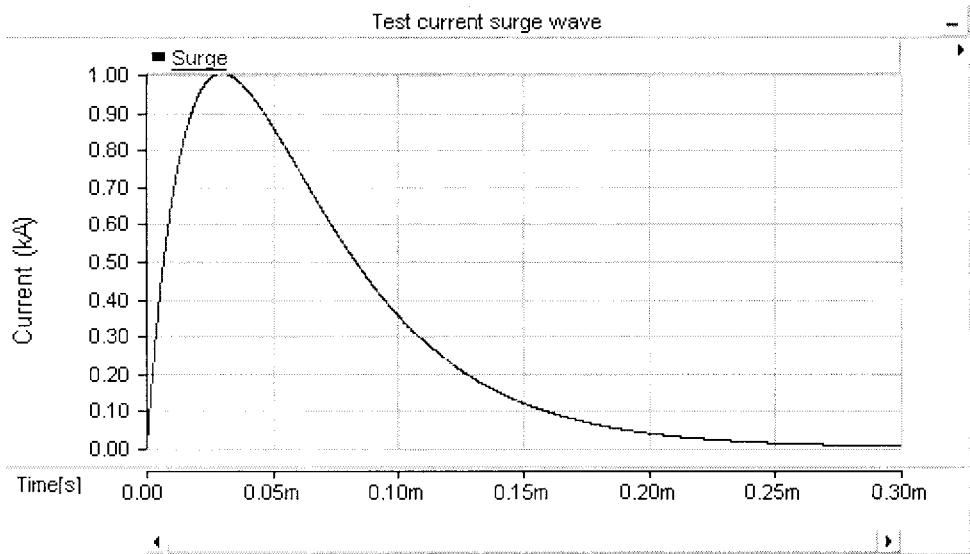


Figure 4.13 – Test surge waveform 30/60 μ s with 1kA peak

The arrester voltage rating (U10/1.6) of only A1 component was changed. A peak value of 357kV discharge voltage was obtained at 270.5kV arrester voltage rating (See Figure 4.14).

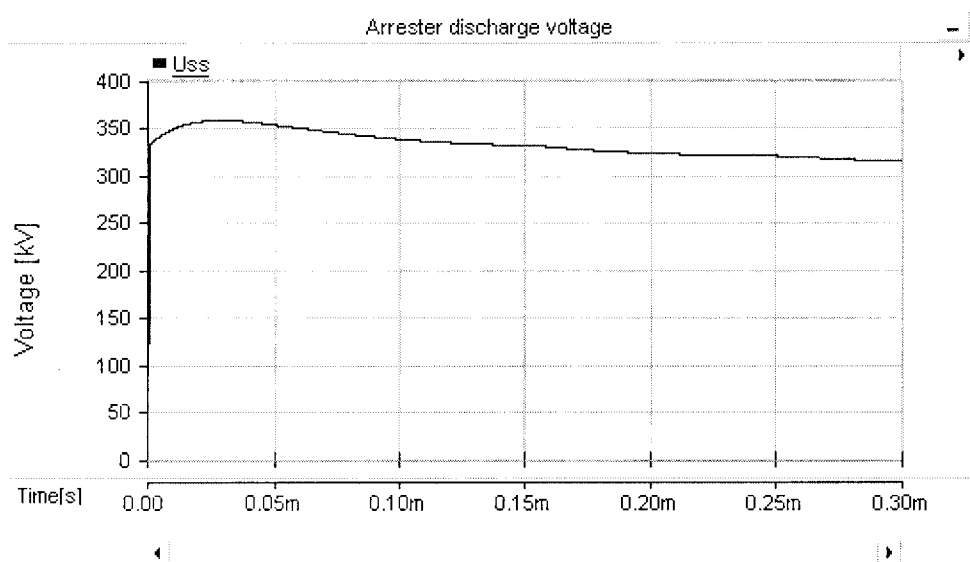


Figure 4.14 – Test result, arrester discharge voltage at 1kA

Step 5:

The arrester model now has correct non-linear resistances for the A_0 and A_1 sections for switching surges. It is now required to test to obtain a good match for the discharge voltage with the $8/20\mu\text{s}$ injected current. The filter inductance L_1 in the model is adjusted until the test circuit produces a good match with the manufacturer's U_{10} discharge voltage.

As per the manufactures' data shown in table 2 of Annex 7,

$U_{10} = 423\text{kV}$ (peak) for 10kA surge of $8/20\mu\text{s}$ wave shape.

Two slider components are used in the test circuit to change the peak current of test surge and the L_1 inductor value as shown in the Figure 4.12.

The same double exponential test surge wave generator circuit is used with different coefficient of exponent values to generate the $8/20\mu\text{s}$ wave as shown in the Figure 4.15.

A value of 423kV peak discharge voltage was obtained by setting the inductance L_1 to $1.795 \times 10^{-5}\text{H}$.

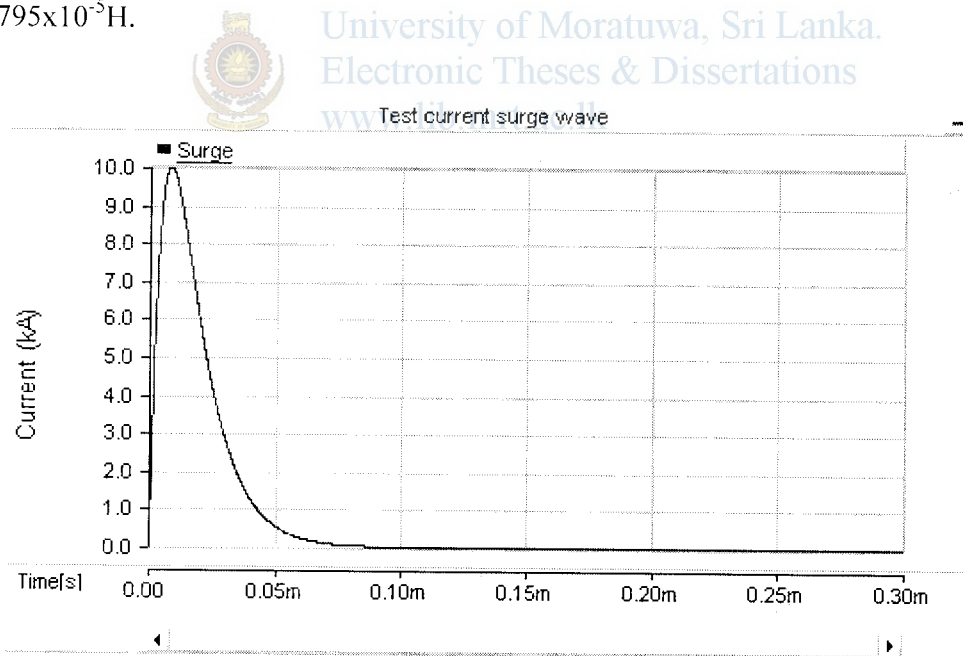


Figure 4.15 – Test surge waveform $8/20\mu\text{s}$ with 10kA peak

The obtained discharge waveform is shown in the Figure 4.16.

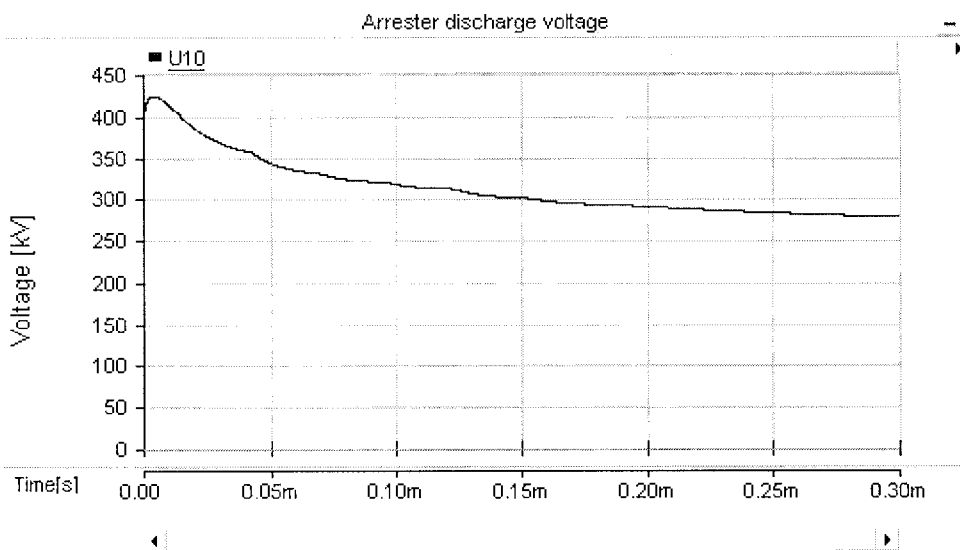


Figure 4.16 – Test result, arrester discharge voltage at 10kA

4.3.8 Lightning surge generator model

As per the equation 3.14 given in the section 3.3.7, the standard 8/20 μ s double exponential waveform was generated by an inbuilt current source having its magnitude controlled by an external control circuit (see the Figure 4.17). The external control circuit consists of two similar parallel branches with a common input parameter component giving the simulation time of the system. Each branch consists of an exponential function component and a multiplier component in series. The multiplier component determines the magnitude of the current waveform which controlled externally by the “Multiple Run” simulation component as described in the section 4.5. As shown in the Figure 4.17, the Differencing junction component gives

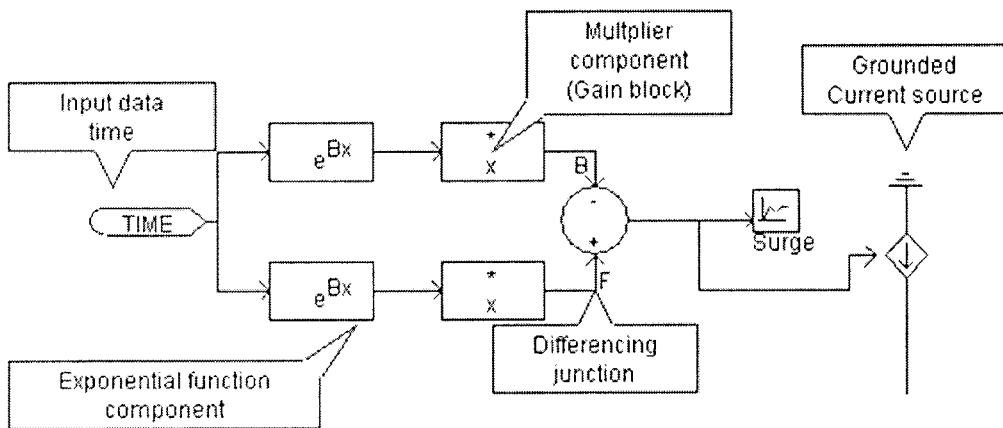


Figure 4.17 – Lightning surge generator model created in PSCAD

the instantaneous values of double exponential waveform to the current source. Current source generates the complete waveform based on the instantaneous values given by the control circuit.

Similarly, a voltage source is used instead of the current source to generate the standard 1.2/50 μ s voltage surge waveform.

4.4 Assembly of sub models and data signal coordination

The sub models described in the previous chapters were created in a single working space named as a page or a module as defined in PSCAD. All the sub models were interconnected by using the wire tool where ever needed to form the complete transient line model as shown in the Figure 3.1.

Inter dependent sub models such as back flashover model and phase voltage generator model were virtually inter connected by giving an identical reference names for each common variables. For an example, the “Phase Voltage” variable is referred as V_a in both phase voltage generator model as well as in the back flashover model. The phase voltage V_a is an output variable produces by the phase voltage generator model whereas it is an input as well for the back flash model in the same time frame.

Similarly the data signals of common variables were managed by assigning them with identical data signal labels.

4.5 Method of simulation

4.5.1 Multiple Run component and variable settings

Simulation of the completed final transmission line model was carried out by using

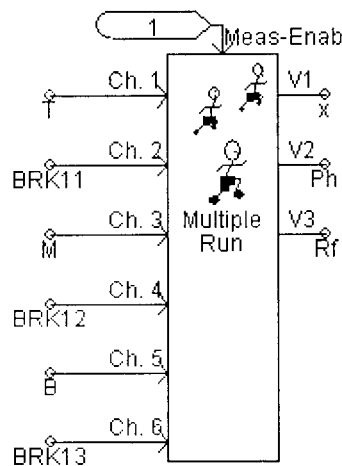


Figure 4.18 – Multiple Run simulation component in PSCAD

the “Multiple Run” simulation component (See Figure 4.18) available in the Master Library of PSCAD. This component can be used to control a multiple run, while manipulating variables from one run to the next. These variables are output from the component (up to six outputs) and can be connected to any other PSCAD components. The Multiple Run component can also record up to six channels each run.

Three (03) numbers of variables those directly affecting the back flashovers were varied in each run of the simulation by using the Multiple Run component. The variables are,

1. Magnitude of the lightning surge current labeled as “x” in the model is set as V1 of Multiple Run component
2. Phase angle of the power frequency phase voltage labeled as “Ph” in the model is set as V2 of Multiple Run component
3. Grounding resistance of Tower-M labeled as “Rf” in the model is set as V3 of Multiple Run component

The range of values set for each variable in the Multiple Run component is shown in the Table 4.2.

Variable in Multiple Run component	Data label used in the model	Range of values
V1	x	30kA to 200kA with 10kA steps
V2	Ph	0^0 to 360^0 with 10^0 steps
V3	Rf	17Ω , 62Ω , 9Ω

Table 4.2 – Range of values used for variables in Multiple Run component

According to [6], the shielding failure flashovers are more frequent at surge current values less than 20kA; whereas the back flashovers take place at higher surge current ratings around 80kA. Therefore a range of values from 30kA to 200kA with 10kA step is selected for the variable “x” as shown in the table 4.2.

Simulations were carried out from 0° to 360° full range of phase angles with a 10° phase angle step to examine the effect of phase angle on back flashovers.

Grounding resistance of the Tower-M (Middle tower which is subjected to the lightning surge as shown in the figure 3.1) is set for one of the three values as shown in the table 4.2 in each simulation.

As shown in Annex-6, the recorded maximum tower grounding resistance even with the soil ionization effect is around 17Ω when the surge current is about 30kA. Therefore the value 17Ω is the recorded worst case of tower grounding resistance with the soil ionization effect and is selected as one of the three values used in the simulations.

As shown in the Figure 1.9, the maximum recorded tower grounding resistance is about 62Ω when the soil ionization effect is not considered. Therefore the value 62Ω is the worst case of tower grounding resistance when the soil ionization effect is neglected. Therefore the value 62Ω is also selected as the second value to be used in the simulations as tower grounding resistance variable V3 as shown in the Table 4.2.

The standard value specified by the local utility for the tower grounding resistance of any transmission line is about 10Ω . Therefore a value less than 10Ω (i.e. 9Ω) is also used in the simulations to investigate the performance of towers against lightning back flashovers.

While changing the value of above variables in each run of the simulations, the control signal output of each back flashover control modules were recorded by the aid of six channel recorders available in the same Multiple Run component. The recorded control signal outputs are stored in an output file assigned to the Multiple Run component. These control signal output data are in binary form where the output “0” means a back flashover event.

4.5.2 Simulation criteria

Simulation of complete line model is carried out in two major steps. At first step, the model is simulated without arresters for selected three (03) critical tower grounding resistance values 9Ω , 17Ω and 62Ω for both $8\times 20\mu\text{s}$ and $1.2\times 50\mu\text{s}$ surge waveforms.

In the second step the model is simulated with surge arresters with two different arrester configurations for both $8\times 20\mu\text{s}$ and $1.2\times 50\mu\text{s}$ surge waveforms. However the

simulations were carried out for above two arrester configurations with only 62Ω tower grounding resistance which is the worst case out of the selected three values.

For all simulations the lightning surge current was injected on top of the Tower M (Middle tower as shown in the Figure 3.1). Detailed criteria of each simulation including the tower grounding resistance setting and expected control signal output data to be recorded are described in the Table 4.3 and Table 4.4.

Step 1: Simulation of the model without arrester protection

Simulation number	Surge waveform	Tower grounding resistance (Ω)	Expected phases where the control signal output data to be recorded
01	8x20μs	9	Tower-M, Circuit-1 and Circuit-2 All six (06) phases
02	8x20μs	17	Tower-M, Circuit-1 and Circuit-2 All six (06) phases
03	8x20μs	62	Tower-M, Circuit-1 and Circuit-2 All six (06) phases
04	1.2x50μs	9	Tower-M, Circuit-1 and Circuit-2 All six (06) phases
05	1.2x50μs	17	Tower-M, Circuit-1 and Circuit-2 All six (06) phases
06	1.2x50μs	62	Tower-M, Circuit-1 and Circuit-2 All six (06) phases

Table 4.3 – Detailed simulation criteria for Step-1

Step 2: Simulation of the model with arrester protection

Simulation number	Surge waveform	Tower grounding resistance (Ω)	Expected phases where the control signal output data to be recorded
<i>With single (01) arrester installed at TOP phase of circuit-2 of Tower-M</i>			
07	8x20μs	62	Tower-M, Circuit-1 and Circuit-2 All six (06) phases
08	1.2x50μs	62	Tower-M, Circuit-1 and Circuit-2 All six (06) phases

<i>With two(02) arresters each one installed at TOP phase of circuit-1&2 of Tower-M</i>			
09	8x20 μ s	62	Tower-M, Circuit-1and Circuit-2 All six (06) phases
10	1.2x50 μ s	62	Tower-M, Circuit-1and Circuit-2 All six (06) phases
11	8x20 μ s	62	Tower-L1, Circuit-1and Circuit-2 All six (06) phases
12	1.2x50 μ s	62	Tower-L1, Circuit-1and Circuit-2 All six (06) phases

Table 4.4 – Detailed simulation criteria for Step-2

4.5.3 Project simulation settings

For each simulation runs, following project simulation settings were assigned.

1. Duration of each run = 70 μ s
2. Solution time step = 0.1 μ s
3. Channel plot step = 0.1 μ s



University of Moratuwa, Sri Lanka.
Electronic Theses & Dissertations
www.lib.mrt.ac.lk

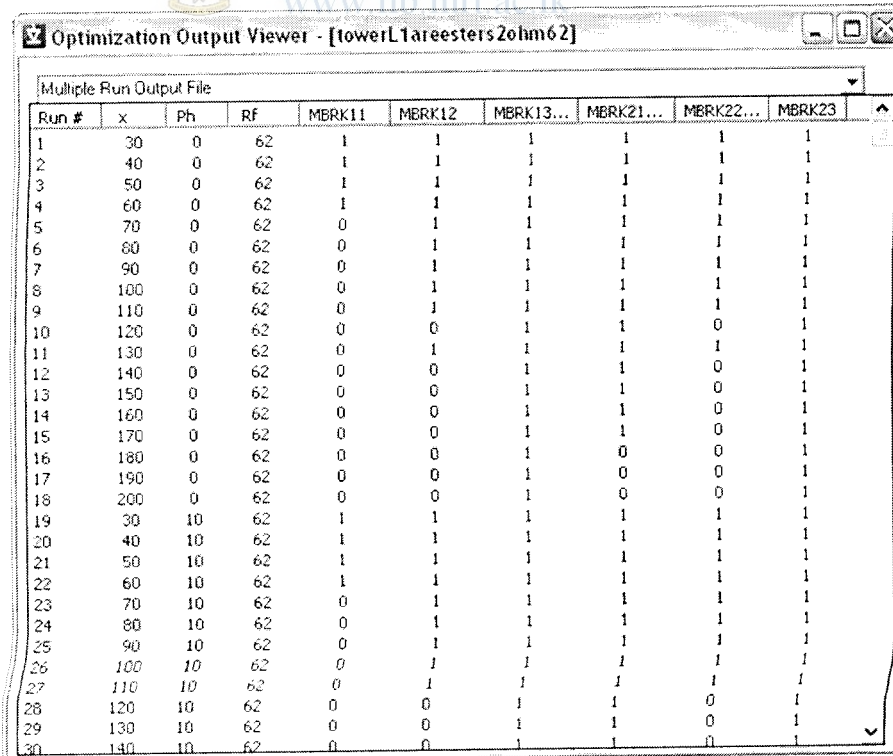
Chapter - 5

Results and analysis

5.1 Introduction

This chapter provides the results of each simulation carried out as per the detailed simulation criteria mentioned in the previous chapter. The results are provided in this chapter as the same sequence of simulations carried out as per the Table 4.3 and Table 4.4.

The results of each simulation are given by an output data file which contains a set of binary values giving the occurrence of back flashover events for each simulation run. The binary value “0” means an occurrence of a back flashover event whereas “1” gives the negation of that event. A typical view of an output data file is shown in the Figure 5.1. As shown in the figure 5.1, the columns MBRK11, MBRK12 and MBRK13 gives the back flashover events occurred on TOP, MIDDLE and BOTTOM phases of circuit-1 of Tower-M respectively. Similarly the columns MBRK21, MBRK22 and MBRK23 gives the back flashover events occurred on TOP, MIDDLE



Run #	x	Ph	RF	MBRK11	MBRK12	MBRK13...	MBRK21...	MBRK22...	MBRK23
1	30	0	62	1	1	1	1	1	1
2	40	0	62	1	1	1	1	1	1
3	50	0	62	1	1	1	1	1	1
4	60	0	62	1	1	1	1	1	1
5	70	0	62	0	1	1	1	1	1
6	80	0	62	0	1	1	1	1	1
7	90	0	62	0	1	1	1	1	1
8	100	0	62	0	1	1	1	1	1
9	110	0	62	0	1	1	1	1	1
10	120	0	62	0	0	1	1	0	1
11	130	0	62	0	1	1	1	1	1
12	140	0	62	0	0	1	1	0	1
13	150	0	62	0	0	1	1	0	1
14	160	0	62	0	0	1	1	0	1
15	170	0	62	0	0	1	1	0	1
16	180	0	62	0	0	1	0	0	1
17	190	0	62	0	0	1	0	0	1
18	200	0	62	0	0	1	0	0	1
19	30	10	62	1	1	1	1	1	1
20	40	10	62	1	1	1	1	1	1
21	50	10	62	1	1	1	1	1	1
22	60	10	62	1	1	1	1	1	1
23	70	10	62	0	1	1	1	1	1
24	80	10	62	0	1	1	1	1	1
25	90	10	62	0	1	1	1	1	1
26	100	10	62	0	1	1	1	1	1
27	110	10	62	0	1	1	1	1	1
28	120	10	62	0	0	1	1	0	1
29	130	10	62	0	0	1	1	0	1
30	140	10	62	0	0	1	1	0	1

Figure 5.1 – Typical view of an output data file

and BOTTOM phases of circuit-2 of Tower-M respectively.

Based on the information provided by the output files of each simulation; the variation of minimum current required for back flashover event were plotted and are produced here as the final results.

5.2 Back flashover minimum current variation results and analysis

5.2.1 Results of simulations without arrester protection (Step-1)

The step-1 consists of six numbers of simulations from simulation no-01 to 06. All these six numbers of simulations were carried out without arrester module for both $8 \times 20 \mu\text{s}$ and $1.2 \times 50 \mu\text{s}$ surge waveforms respectively. Further above simulations were

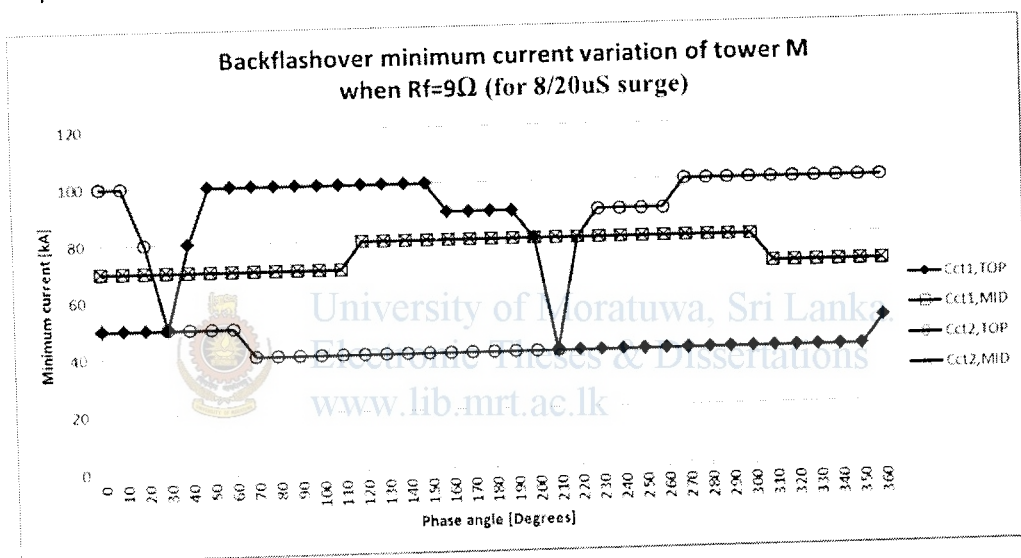


Figure 5.2 – Results of simulation no.1

also done by applying selected 9Ω , 17Ω and 62Ω tower grounding resistances values.

As per the results shown in Figure 5.2(Simulation no.01) and Figure 5.4(Simulation no.02) it can be seen clearly that the results are almost same for $8 \times 20 \mu\text{s}$ current surge for both tower grounding resistances of 9Ω and 17Ω . However the results for the 62Ω tower grounding resistance with $8 \times 20 \mu\text{s}$ current surge as shown in the Figure 5.6 (Simulation no.03) is different than the first two results.

Similarly as per the Figures 5.3(Simulation no.04), 5.5(Simulation no.05) and Figure 5.7(Simulation no.06) it can be seen a clear similarity of the results given for the $1.2 \times 50 \mu\text{s}$ surge waveform for 9Ω , 17Ω and 62Ω tower grounding resistances.

All the results from simulation no.01 to 06 except the results of simulation no.03 shows that the lowest back flashover minimum current (=40kA) is recorded in the TOP phases of the both circuits. However the TOP phase of circuit-2 was flashover at 40kA only for the phase angles ranging from 60° to 200° whereas the TOP phase of the other circuit was flashover at same 40kA current only in the phase angles ranging

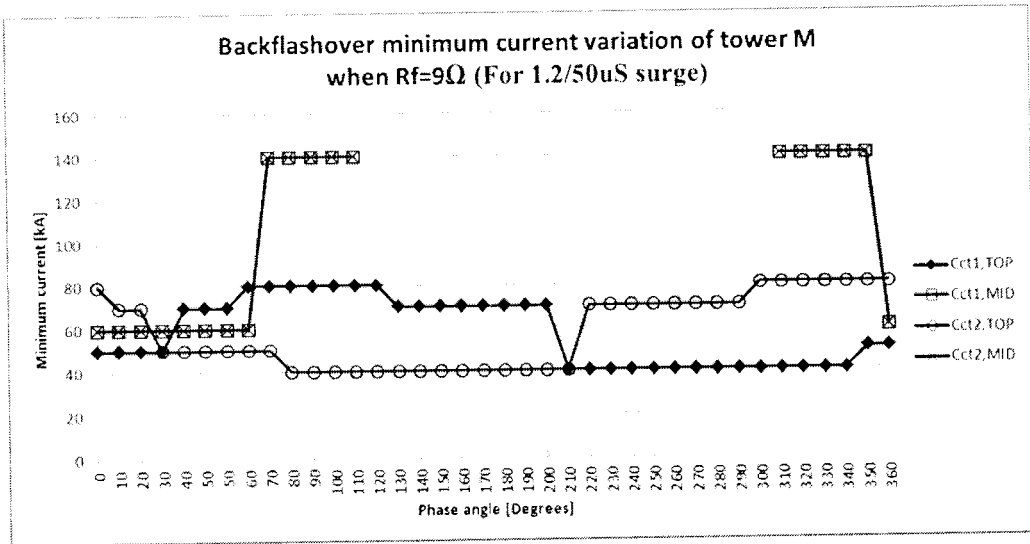


Figure 5.3 – Results of simulation no. 4

from 200° to 340° . (See Figures 5.2, 5.3, 5.4, 5.5 and 5.7) Further from the above result shows that when the phase angle changes from 200° to 210° the back flash over event also changes from TOP phase of circuit-02 to TOP phase of the other circuit at 40kA surge current.

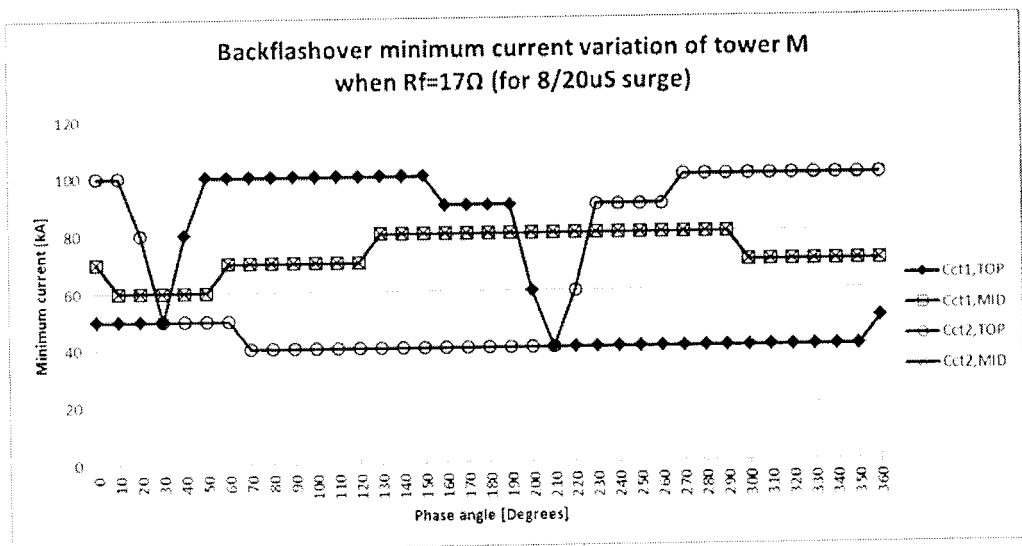


Figure 5.4 – Results of simulation no. 2

As per the results shown in the Figure 5.6 (Simulation no. 3) it shows that the MIDDLE phases and the TOP phases of both circuits are having the same lowest back flashover minimum current at 62Ω for $8 \times 20\mu\text{s}$ surge. However the TOP phases of

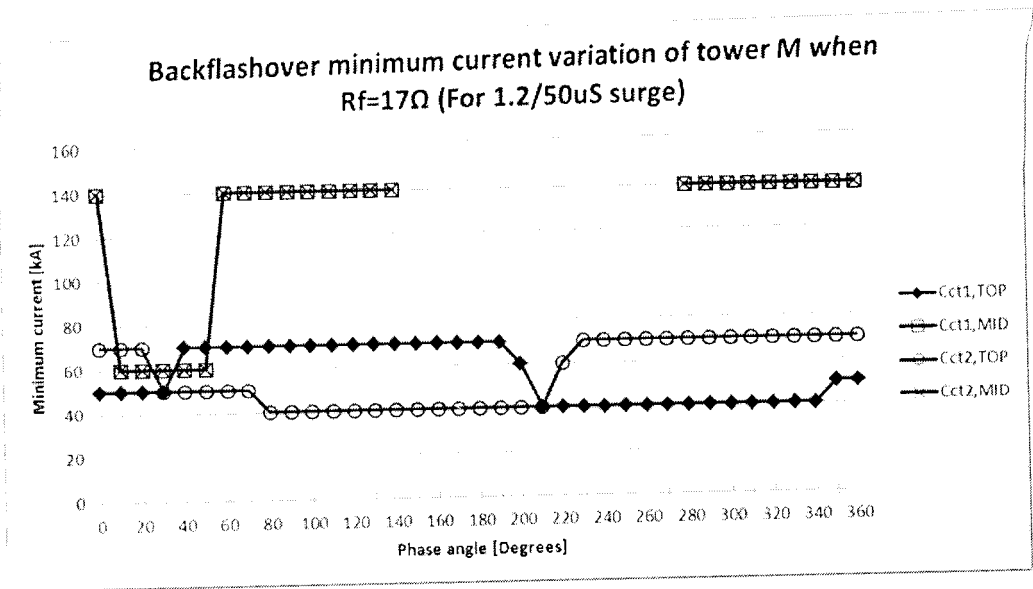


Figure 5.5 – Results of simulation no. 5

both circuits are not having the same lowest current at once at the same phase angle except at 30° and 210° .

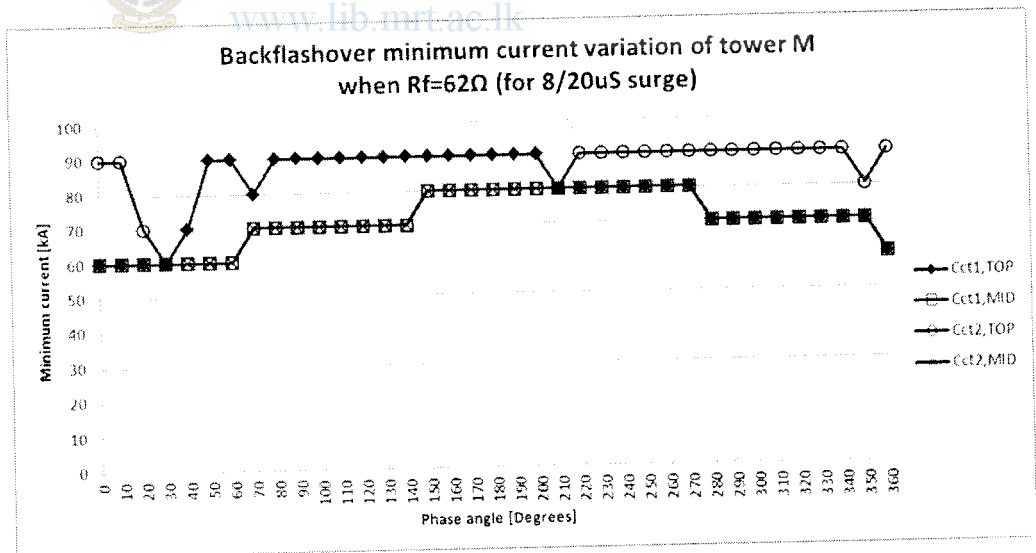


Figure 5.6 – Results of simulation no. 3

There is no back flashover events were recorded in the BOTTOM phases in any of the simulations done without arrester module. Therefore it is clear that the TOP and MIDDLE phase are more likely to have back flashovers than any of the BOTTOM phases.

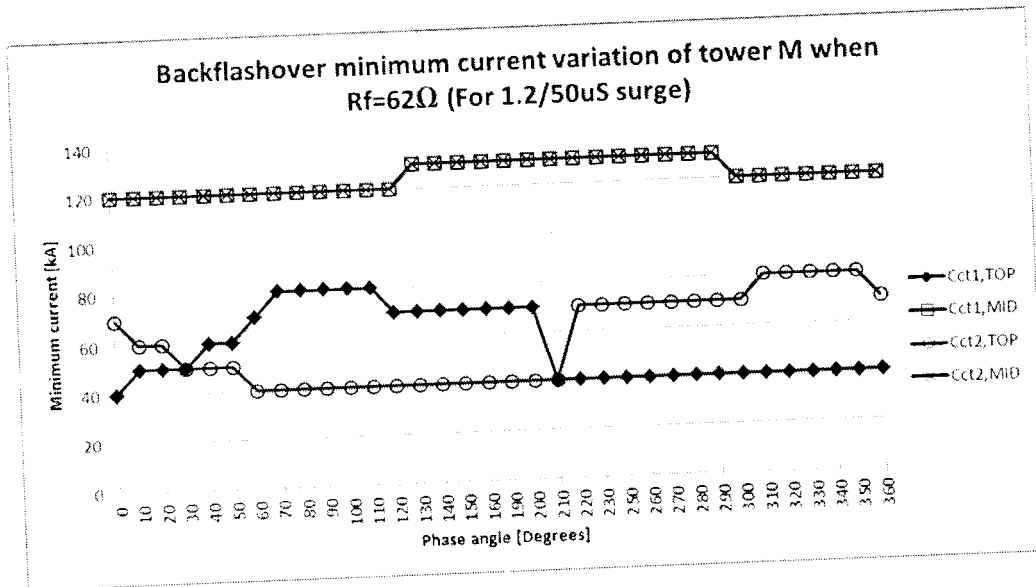


Figure 5.7 – Results of simulation no. 6

5.2.2 Results of simulations with arrester protection (Step-2)

Arrester configuration-1: Single arrester installed on TOP phase of circuit-2 of Tower-M

As per the Figures 5.8 and 5.9, the results of the simulations done with single arrester configuration are almost same for the TOP phase of circuit-01 for both 8x20μs and 1.2x50μs surge waveforms. Few back flashover events were recorded in the MIDDLE

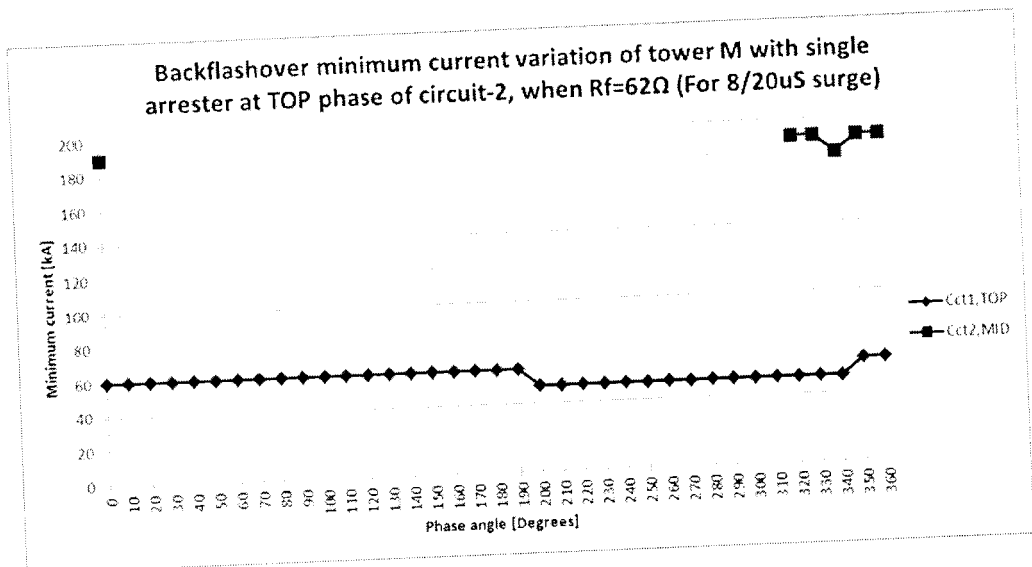


Figure 5.8 – Results of simulation no. 7

phase of the circuit 2 for only $8 \times 20 \mu\text{s}$ surge waveform at phase angle 0° and from 320° to 360° at 180/190kA. The lowest back flashover minimum current of the TOP phase of the circuit -01 is about 50kA when the phase angle ranging from 200° to 340° .

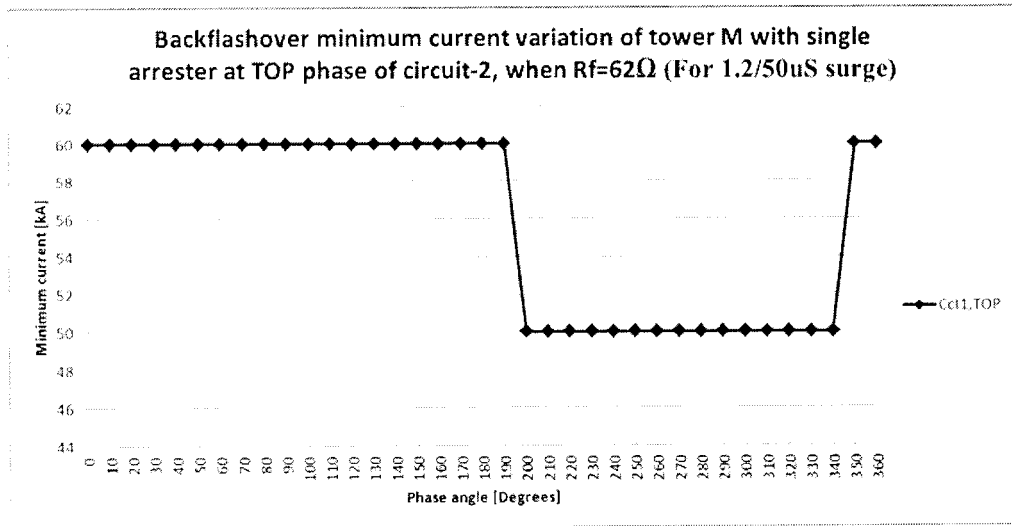


Figure 5.9 – Results of Simulation no. 8

However the back flashovers are recorded in the TOP phase of circuit-01 and the MIDDLE phase of circuit-02 only. Therefore it is clearly shows that the arrester installed in the TOP phase of the circuit-02 provides the protection against back flashovers as follows.

1. Protects the same phase (i.e. TOP phase of circuit-02) up to 200kA
2. Protects the TOP phase of circuit-01 up to 50kA
3. BOTTOM and MIDDLE phases of circuit-01 up to 200kA
4. BOTTOM phase of circuit -02 up to 200kA and MIDDLE phase up to 180kA

Arrester configuration-2: Two (02) arresters each installed on TOP phase of circuit-1 and circuit-2 of Tower-M

As per the results of simulation no. 09 and 10 (with two arrester configuration), it is clearly noticed that there is no back flashovers occurs on any phase of the Tower-M

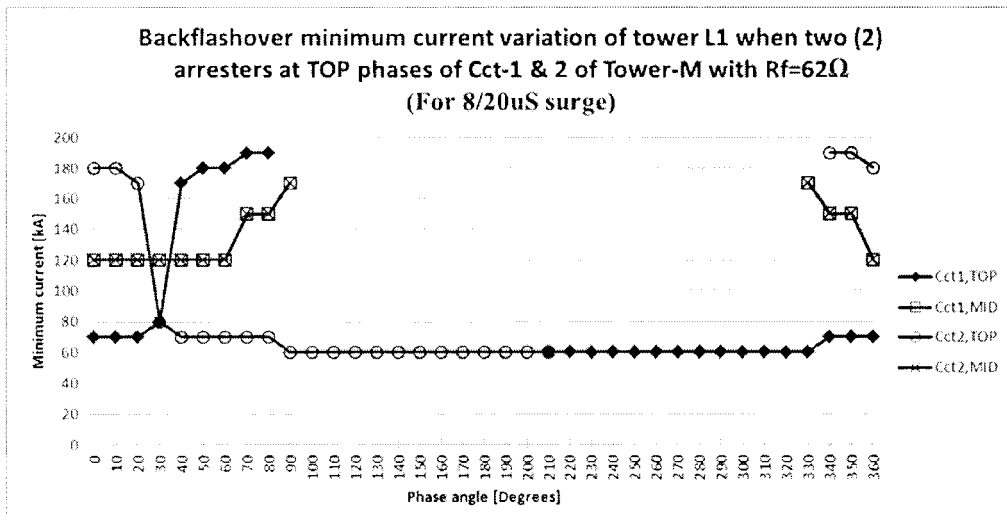


Figure 5.10 – Results of Simulation no. 11

for any of the selected three tower grounding resistance values for both surge waveforms. Therefore two arrester configuration of Tower M provides the full protection against back flashovers for all phases of the same tower.

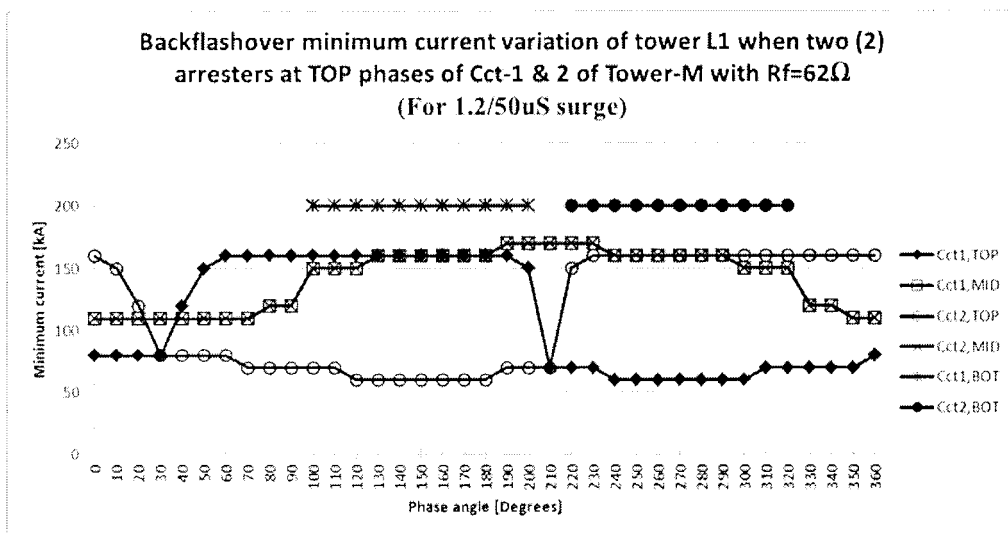


Figure 5.11 – Results of Simulation no. 12

However the results given in the Figure 5.10 and 5.11 shows that back flashover events were recorded in almost all phases of both circuits of the adjacent tower L1

even if the grounding resistance of tower M is at 62Ω for both surges. Therefore the two arrester configuration at Tower M is not providing the protection against back flashovers for the adjacent towers.



University of Moratuwa, Sri Lanka.
Electronic Theses & Dissertations
www.lib.mrt.ac.lk

Chapter - 6

Conclusion and recommendations

6.1 Conclusion

Almost all simulations carried out without arrester protection (Step-1) shows that the TOP phase of each circuit has a lower back flashover minimum current value compared to the rest of the phases. Therefore it can be concluded that the TOP phases of each circuit are more likely to have back flashovers compared to the rest of the phases.

As per the results given for the simulations, carried out with single arrester installed in TOP phase of circuit-02 (Step-2) gives no protection for the TOP phase of the other circuit beyond 50kA surges. However all phases of the circuit-02 is protected up to 200kA except the MIDDLE phase which is only up to 180kA.

According to the results of the simulations carried out with two (02) arrester configuration, it is observed that the protection against back flashovers is provided only for the tower installed with two (02) arresters at its TOP phases. Further it is noted that the adjacent side towers are not protected against back flashovers by the arresters installed on the tower at the middle. Therefore each tower needs to be protected individually.

6.2 Recommendations

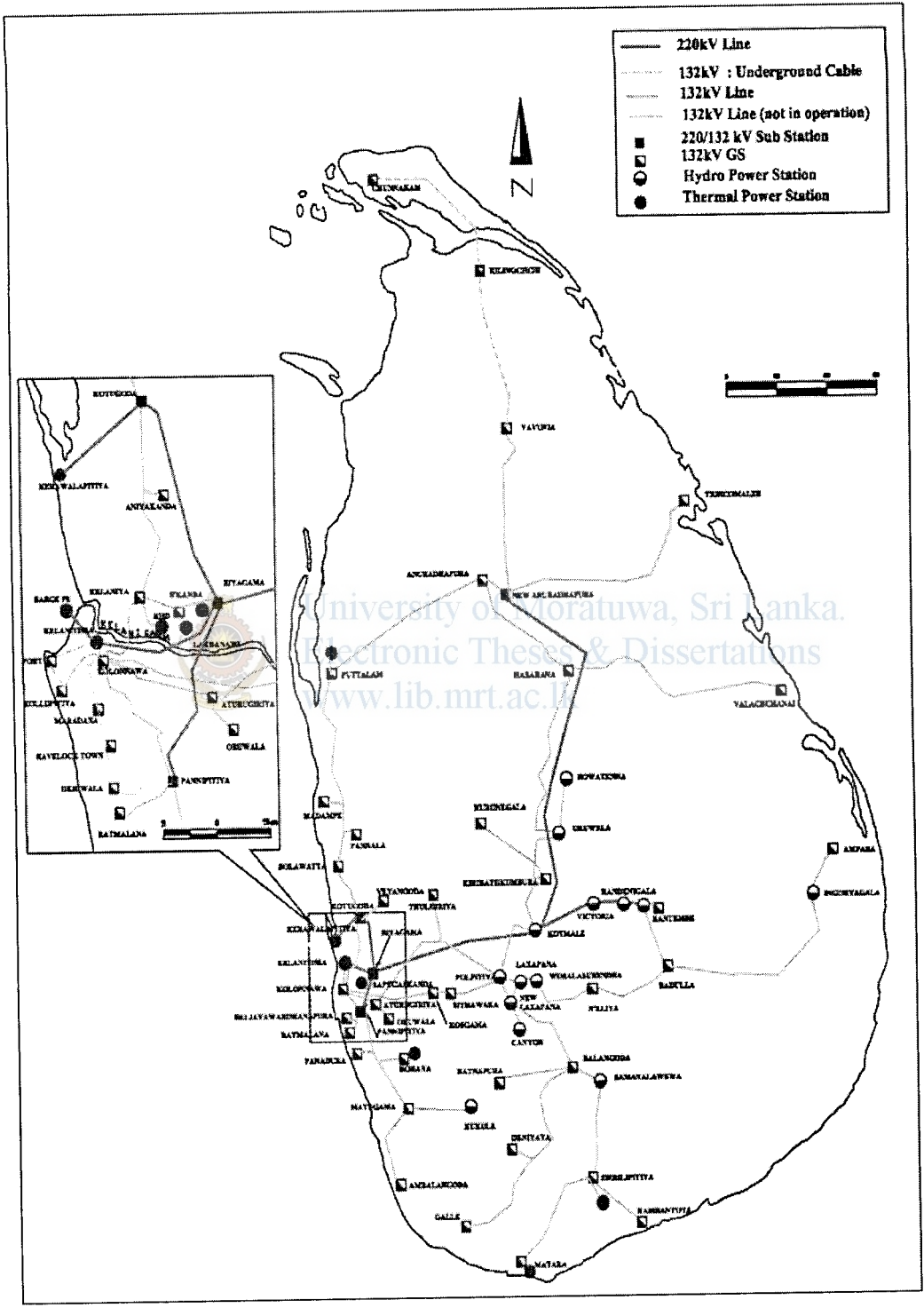
According to the conclusions described in the previous section, initially it can be recommended to install 02nos. of Transmission Line Arresters (TLAs) each on TOP phases of each tower from tower no.33 to 50 and tower no.85-95 where the most insulator damages are recorded.

The selection and matching of mechanical characteristics of Transmission Line Arresters to the system characteristics and maintenance requirements has to be done to complete the full selection procedure as described in the section 3.4.

References

- [1] Vladimir A. Rakov and Martin A. Uman, *Lightning Physics and Effects*, Cambridge: Cambridge University Press, 2003, [E-Book]
Available: <http://www.cambridge.org>, [Accessed: 22nd September 2010]
- [2] A. Morched, B. Gustavsen, M. Tartibi, *A Universal Line Model for Accurate Calculation of Electromagnetic Transients on Overhead Lines and Cables*, Paper PE-112-PWRD-0-11-1997
- [3] J. Rohan Lucas, *High Voltage Engineering*, Revised edition 2001, Open University of Sri Lanka, Open University Press, 2001
- [4] K.S.S. Kumara, "Lightning Performance of Sri Lankan Transmission Lines: A Case Study", M.Sc. thesis, University of Moratuwa, Katubedda, Sri Lanka, 2009
- [5] Gi-ichi Ikeda, "Report on Lightning Conditions in Ceylon, and Measures to Reduce Damage to Electrical Equipment", Asian Productivity Project TES/68, 1969
- [6] EPRI, "Handbook for Improving Overhead Transmission Line Lightning Performance", EPRI, Palo Alto, CA: 2004. 1002019
- [7] M. Kizilcay, C. Neumann, "Back Flashover Analysis for 110kV Lines at Multi-Circuit Overhead Line Towers", *International Conference on Power Systems Transients (IPST'07) in Lyon, France on June 4-7, 2007*
- [8] Canadian/American EMTP User Group: *ATP Rule Book*, Distributed by the European EMTP-ATP Users Group Association, 2005
- [9] Chisholm, W. A.; Chow, Y. L.; Srivastara, K.D: "Travel Time of Transmission Towers", *IEEE Trans. on Power App. And Systems*, Vol. PAS-104, No. 10, S.2922-2928, October 1985
- [10] CIGRE WG 33-01: "Guide to Procedures for Estimating the Lightning Performance of Transmission Lines", Technical Brochure, October 1991.
- [11] Manitoba HVDC Research Centre, "Applications of PSCAD/EMTDC", Application Guide 2008, Manitoba HVDC Research Centre Inc., Canada
- [12] IEEE Working Group 3.4.11, "Modeling of Metal Oxide Surge Arresters," *IEEE Transactions of Power Delivery*, Vol. 7, No.1, January 1992, pp 302-309
- [13] ABB, "High Voltage Surge Arresters" Buyer's Guide 2008-08, Ed.6, ABB AB, Sweden

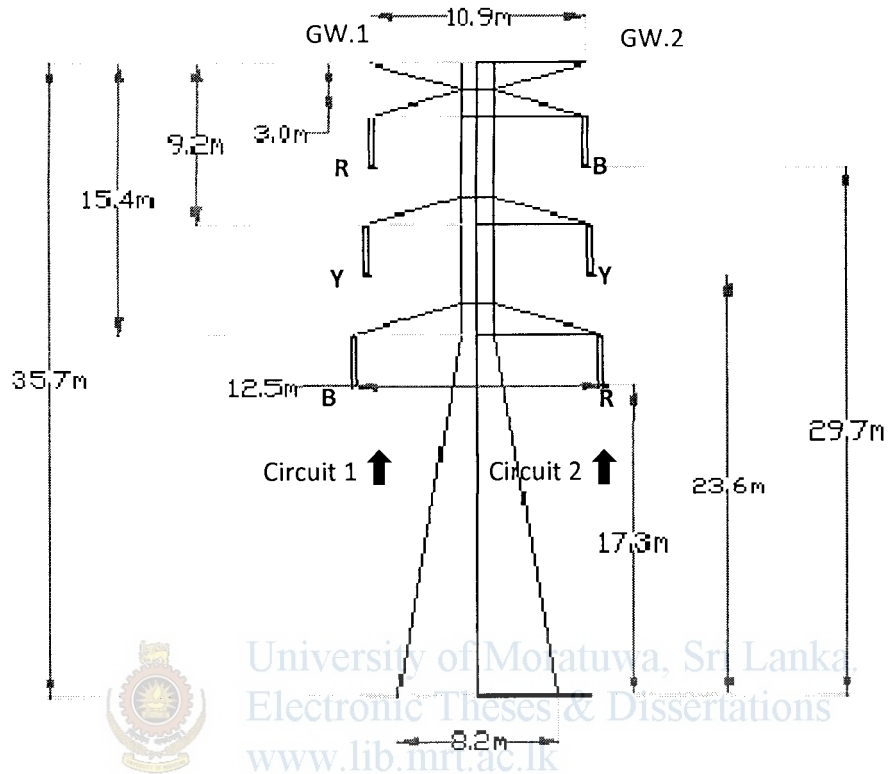
Annex-1 Present Transmission system of Sri Lanka



Annex-3 220kV Biyagama – Kotmale transmission line parameters

#	Line parameters' description	Value	Unit	Comment
1	Voltage	220	kV	
2	Steady state Frequency	50	Hz	
3	Line/Span length	As per the tower schedule (Annex 5)	Km	
4	Line shunt conductance	1×10^{-11}	m Ω /m	
5	No. of circuits	02	Nos.	
6	Conductor Type/Name	ACSR "ZEBRA"		
7	Conductor size	428.9	mm ²	
8	Conductor radius	0.01431	m	
9	Conductor DC resistance	0.0674	Ω /km	
10	Sag of all phase conductors	9.56	m	
11	No. of sub conductors per phase	02	Nos.	
12	Bundle configuration	Symmetrical		
13	Sub conductor spacing	0.4	m	
14	Earth wire Type/Name	GS 7/3.25		
15	Earth wire size	58.07	mm ²	
16	No. of Earth wires	02	Nos.	
17	Earth wire radius	0.0049	m	
18	Earth wire DC resistance	3.1	Ω /km	
19	Sag of Earth wire	6.41	m	
20	Ground resistivity	1000	Ω m	
21	Relative ground permeability	1.0		
Other parameters used in the Transmission line model				
22	Conductor coordinates reference to the center of the tower base			
23	Phase/nodal connection information of line interface			
24	Ideally transposed line?			YES

Annex-4: A typical transmission tower used in the selected transmission line



Annex-5: Tower schedule

Tower number	Span/Line Section length (m)	Tower type	Tower height(m)
1 to 32	12,088		
33	333	1D1	34.885
34	458	1D3	34.710
35	285	1DL	35.741
36	174	1DL	35.741
37	488	1DL	35.741
38	232	1D1	34.885
39	258	1D1	34.885
40	438	1D6+6	40.710
41	287	1D6+6	40.710
42	506	1DL+9	44.741
43	297	1D3+3	37.710
44	186	1DL+6	41.741
45	376	1DL	35.741
46	568	1D1+6	40.885
47	239	1DL+3	38.741
48	261	1D6	34.710
49	329	1DL+6	41.741
50	261	1DL+9	44.741
50 to 84	11,999		
85	181	1D6	34.710
86	682	1D1	34.885
87	474	1D1	34.885
88	422	1D1+3	37.885
89	356	1D1	34.885
90	513	1DL	35.741
91	281	1D3	34.710
92	692	1D1	34.885
93	397	1D1	34.885
94	477	1D1	34.885
95	477	1D1	34.885
95 to 206	35,525		

Annex-6 Grounding Resistance variation of towers due to soil ionization effect

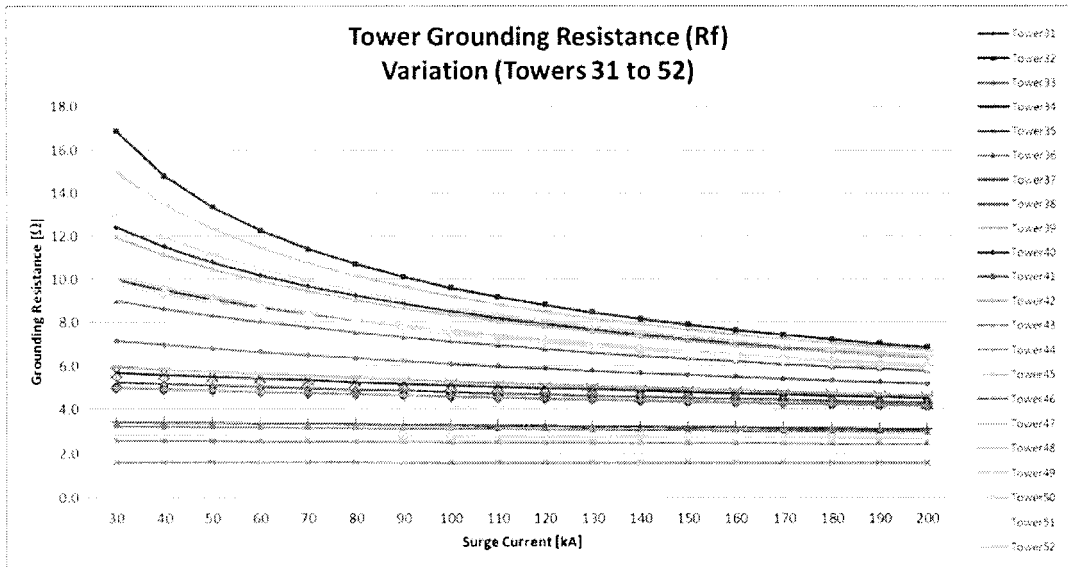


Figure A6-1: Grounding resistance variation of towers 31 to 52

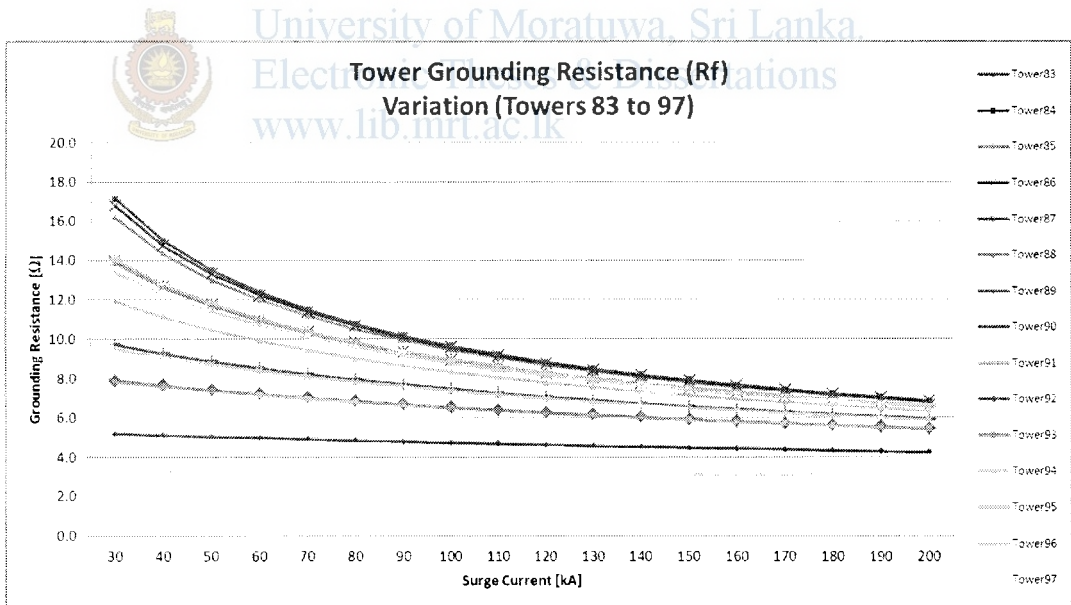


Figure A6-2: Grounding resistance variation of towers 83 to 97

Annex-7 Simplified selection procedure of an ABB surge arrester

Selection of electrical parameters as per the selection procedure shown in Figure 3.12:

Product range

Product family	Arrester classification ¹⁾	Type	Max. system voltage ²⁾	Rated voltage ²⁾	Energy requirement/ Lightning intensity	Mechanical strength ³⁾
			U _m kV _{rms}	U _r kV _{rms}		Nm
PEXLIM — Silicone polymer-housed arresters Superior where low weight, reduced clearances, flexible mounting, non-fragility and additional personnel safety is required Major component for PEXLINK™ concept for transmission line protection.	10 kA, IEC class 2	PEXLIM R	24 - 170	18 - 144	Moderate	1 600
	10 kA, IEC class 3	PEXLIM Q	52 - 420	42 - 360	High	4 000
	20 kA, IEC class 4	PEXLIM P	52 - 420	42 - 360	Very high	4 000
	20 kA, IEC class 4	HS PEXLIM P	245 - 550	180 - 444	Very high	28 000
HS PEXLIM - High strength silicone polymer-housed arresters. Specially suited to extreme seismic zones.	20 kA, IEC class 5	HS PEXLIM T	245 - 600	180 - 612	Very high	28 000
	10 kA, IEC class 2	EXLIM R	52 - 170	42 - 168	Moderate	7 500
EXLIM — Porcelain-housed arrester	10 kA, IEC class 3	EXLIM Q-E	52 - 245	42 - 228	High	7 500
	10 kA, IEC class 3	EXLIM Q-D	170 - 420	132 - 420	High	18 000
	20 kA, IEC class 4	EXLIM P	52 - 550	42 - 444	Very high	18 000
	20 kA, IEC class 5	EXLIM T	245 - 600	180 - 624	Very high	18 000

¹⁾ Arrester classification according to IEC 60399-4 (nominal discharge current, line discharge class).
²⁾ Arresters with lower or higher voltages may be available on request for special applications.
³⁾ Specified short-term service load (SSL).

Table A7-1: Product range of ABB Surge arresters [13]

Step 1: Selection of rated voltage (U_r)

System voltage (U_m) = 245kV, System earthing = effectively earthed, Earth fault duration ≤ 1s (Maximum 1.5s for backup protection) Therefore from Table A7-3,

Rated voltage, $U_r \geq 0.72 \cdot U_m$

$$U_r \geq 176.4 \text{ kV}$$

The Table A7-3 gives a minimum value of the arrester rated voltage (U_r). In each case, choose the next higher standard rating as given in the catalogue (Table A7-2). ABB Transmission Line Arresters (TLA) uses PEXLIM-Q Metal Oxide Surge Arresters as the arrester component. Table A7-2 gives the protective data of PEXLIM Q type arresters.

Therefore, $U_r = 180 \text{ kV}$ from table 2 (for PEXLIM Q arrester type)

Step 2: Selection of line discharge class and energy capability

From Table A7-4, for PEXLIM Q type arresters

Line Discharge Class = 3 and Energy capability = 7.8kJ/kV (U_r) for $U_m = 170$ -420kV range

Max. System Voltage U_m kV _{rms}	Rated Voltage U_r kV _{rms}	Max. continuous operating voltage 1)		TOV capability 2)		Max. residual voltage with current wave							
		as per IEC		as per ANSI/IEEE		30/60 μ s				8/20 μ s			
		U_c kV _{rms}	MCOV kV _{rms}	1 s kV _{rms}	10 s kV _{rms}	0.5 kA kV _{peak}	1 kA kV _{peak}	2 kA kV _{peak}	5 kA kV _{peak}	10 kA kV _{peak}	20 kA kV _{peak}	40 kA kV _{peak}	
170	132	106	106	151	145	254	262	272	295	311	342	382	
	144	108	115	165	158	277	296	297	322	339	373	417	
	150	108	121	172	165	288	298	309	335	353	388	434	
	162	108	131	186	178	312	321	334	362	381	419	469	
	168	108	131	193	184	323	333	346	376	395	435	485	
	192	108	152	220	211	369	381	396	429	452	497	555	
245	190	144	144	207	199	346	357	371	402	423	466	521	
	192	154	154	220	211	359	381	396	429	452	497	555	
	198	156	160	227	217	381	393	408	443	466	512	573	
	210	156	170	241	231	404	417	433	469	494	543	608	
	216	156	175	248	237	415	428	445	483	508	559	625	
	219	156	177	251	240	421	434	451	489	515	567	634	
	222	156	179	255	244	427	440	458	496	522	574	642	
	228	156	180	252	250	438	452	470	510	536	590	660	
	300	216	173	175	249	237	415	428	445	483	509	559	625
		240	191	191	276	264	461	476	495	536	564	621	694
258		191	209	296	283	496	512	532	576	607	667	746	
264		191	212	303	290	507	523	544	590	621	683	764	
276		191	220	317	303	530	547	569	617	649	714	798	
362		258	206	209	295	283	496	512	532	576	607	667	746
	264	211	212	303	290	507	523	544	590	621	683	764	
	276	221	221	317	303	530	547	569	617	649	714	798	
	288	230	230	331	316	553	571	593	643	677	745	833	

Table A7-2: Guaranteed protective data for ABB PEXLIM Q surge arresters [13]

Step 3: Selection of Lightning and Switching protection levels (U_{pl} and U_{ps})

System Earthing	Fault Duration	System Voltage U_m (kV)	Min. Rated Voltage, U_r (kV)
Effective	≤ 1 s	≤ 100	$\geq 0.8 \times U_m$
Effective	≤ 1 s	≥ 123	$\geq 0.72 \times U_m$
Non-effective	≤ 10 s	≤ 170	$\geq 0.91 \times U_m$ $\geq 0.93 \times U_m$ (EXLIM T)
Non-effective	≤ 2 h	≤ 170	$\geq 1.11 \times U_m$
Non-effective	> 2 h	≤ 170	$\geq 1.25 \times U_m$

Table A7-3: Minimum arrester rated voltages [13]

System parameters for U_{wl} and U_{ws} ,

Lightning withstand voltage of the line $U_{wl} = 1,050\text{kV}$

Switching withstand voltage of the line $U_{ws} = 460\text{kV}$

For insulation co-ordination purposes, consider the lightning impulse protection level (U_{pl}) at 10 kA for $U_m \leq 362$ kV and at 20 kA for higher voltages. Similarly, the switching impulse protection levels (U_{ps}) for co-ordination purposes range from 0.5kA (for $U_m \leq 170$ kV) to 2 kA (for $U_m \geq 362\text{kV}$).

From Table A7-5, for PEXLIM Q arresters at Nominal Discharge Current $I_n = 10\text{kA}$

$U_{pl}/U_r = 2.350$ and $U_{ps}/U_r = 1.981$

Therefore arrester parameters for U_{pl} and U_{ps}

$$U_{pl} = 2.350 * 180\text{kV} = 423\text{kV}$$

$$U_{ps} = 1.981 * 180\text{kV} = 357\text{kV}$$

Arrester Type	Line discharge class	Energy capability (2 impulses) kJ/kV (U_r)	Normal application range (U_m)
EXLIM R	2	5.0	≤ 170 kV
PEXLIM R	2	5.1	≤ 170 kV
EXLIM Q	3	7.8	170 - 420 kV
PEXLIM Q	3	7.8	170 - 420 kV
EXLIM P	4	10.8	362 - 550 kV
PEXLIM P	4	12	362 - 550 kV
HS PEXLIM P	4	10.5	362 - 550 kV
EXLIM T	5	15.4	420 - 800 kV
HS PEXLIM T	5	15.4	420 - 800 kV

Table A7-4: Energy capability of arresters [13]

Step 4: Calculation of protection margins

$$\begin{aligned} \text{Protection margin for lightning impulses} &= \{(U_{wl}/U_{pl}) - 1\} * 100\% \\ &= \{(1050/423) - 1\} * 100\% \\ &= 148\% \end{aligned}$$

$$\begin{aligned} \text{Protection margin for switching impulses} &= \{(U_{ws}/U_{ps}) - 1\} * 100\% \\ &= \{(460/357) - 1\} * 100\% \end{aligned}$$

Arrester Type	Nom. Dis-charge current (I_n)	U_{pl}/U_r at 10 kAp	U_{pl}/U_r at 20 kAp	U_{ps}/U_r
EXLIM R	10	2.590		2.060 at 0.5 kAp
PEXLIM R	10	2.590		2.060 at 0.5 kAp
EXLIM Q	10	2.350		1.981 at 1.0 kAp
PEXLIM Q	10	2.350		1.981 at 1.0 kAp
EXLIM P	20	2.275	2.5	2.020 at 2.0 kAp
PEXLIM P	20	2.275	2.5	2.020 at 2.0 kAp
HS PEXLIM P	20	2.275	2.5	2.020 at 2.0kAp
EXLIM T	20	2.200	2.4	1.976 at 2.0 kAp

Table A7-5: U_{pl} and U_{ps} ratios for ABB arresters [13]

Summary of system and arrester electrical parameters

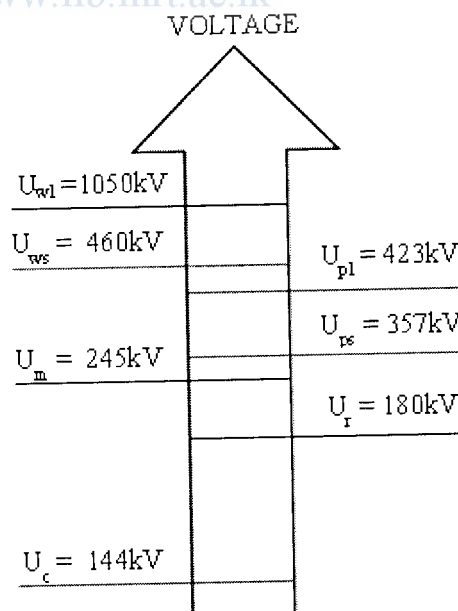


Table A7-6: Summary of system and arrester electrical parameters